DISCLAIMER

This report was prepared as an account of work sponsored by an agency of the United States Government. Neither the United States Government nor any agency thereof, nor any of their employees, makes any warranty, express or implied, or assumes any legal liability or responsibility for the accuracy, completeness, or usefulness of any information, apparatus, product, or process disclosed, or represents that its use would not infringe privately owned rights. Reference herein to any specific commercial product, process, or service by trade name, trademark, manufacturer, or otherwise does not necessarily constitute or imply its endorsement, recommendation, or favoring by the United States Government or any agency thereof. The views and opinions of authors expressed herein do not necessarily state or reflect those of the United States Government or any agency thereof. Reference herein to any social initiative (including but not limited to Diversity, Equity, and Inclusion (DEI); Community Benefits Plans (CBP); Justice 40; etc.) is made by the Author independent of any current requirement by the United States Government and does not constitute or imply endorsement, recommendation, or support by the United States Government or any agency thereof.

Feasibility Analyses for the Microgrid of the Mountain in the Cordillera Central Region of Puerto Rico

Communities Local Energy Action Program (LEAP)
U.S. Department of Energy
January 2026

1st Anjan Debnath
Grid Integration & Control Group
Idaho National Laboratory, ID, USA
anjan.debnath@inl.gov

2nd Timothy McJunkin
Grid Integration & Control group
Idaho National Laboratory, ID, USA
timothy.mcjunkin@inl.gov

3rd Jimmy E. Quiroz
Resilient Energy & Distributed Systems
Sandia National Laboratories, NM, USA
jequiro@sandia.gov

4th Melissa Louie
Risk & Reliability Analyses
Sandia National Laboratories, NM, USA
mlouie@sandia.gov

5th Rachid Darbali-Zamora
Resilient Energy & Distributed Systems
Sandia National Laboratories, NM, USA
rdarbal@sandia.gov

SAND2026-16656R
INL/RPT-25-88335 Rev:000

Feasibility Analyses for the Microgrid of the Mountain in the Cordillera Central Region of Puerto Rico

Anjan Debnath
Grid Integration & Control Group
Idaho National Laboratory, ID, USA
anjan.debnath@inl.gov

Timothy McJunkin
Grid Integration & Control group
Idaho National Laboratory, ID, USA.
timothy.mcjunkin@inl.gov

Jimmy E. Quiroz
Resilient Energy & Distributed Systems
Sandia National Laboratories, NM, USA
jequiro@sandia.gov

Melissa Louie
Risk & Reliability Analyses
Sandia National Laboratories, NM, USA
mlouie@sandia.gov

Rachid Darbali-Zamora
Resilient Energy & Distributed Systems
Sandia National Laboratories, NM, USA
rdarbal@sandia.gov

***Abstract*— Distributed energy resource (DER) development can benefit communities through improvement of access to reliable electricity and a resilient energy system. Many place-specific considerations must be accounted for when designing electrical systems with co-located generation and loads. This paper presents an overview of four studies focusing on different aspects for regional DER development in the Cordillera Central region of Puerto Rico, including a grid and load stability study with the introduction of solar energy generation, microgrid design based on the solar resource in the area, resilience considerations during power outage scenarios, and qualitative risk aspects for components in the microgrid. Additionally, a conceptual substation microgrid analysis is conducted using the Microgrid Design Toolkit (MDT) to evaluate trade-offs between cost and energy availability, providing insights into optimal design strategies. A microgrid resilience assessment is performed using the Resilient Nodal Cluster Analysis Tool (ReNCAT) to identify critical loads and evaluates their accessibility during outages, emphasizing the importance of community needs. Finally, a qualitative risk assessment utilizing Hazard and Operability Analysis (HAZOP) methods highlights potential hazards and mitigations for microgrid components, ensuring robust system design and operation.**

Keywords—Microgrid, Voltage Regulation, PV-Inverter control, Reactive Power, Droop Curve, Design-Basis Threats, Resilience, Risk Mitigation, HAZOP

I. Introduction

For regions where the electrical grid is vulnerable to power outages or other disturbances resulting in intermittent or unreliable electrical service, development of independent, community-owned microgrids can help improve system reliability and resilience. Many factors and priorities must be considered when designing and operating a microgrid, such as energy generation assets and resources, loads, geographical connectivity, existing infrastructure, economic viability, and accessibility. These critical services can include facilities such as utilities (e.g., water, electricity), grocery stores or supermarkets, medical care centers (e.g., hospitals, clinics), and emergency muster points or community centers.

The Cooperativa Hidroeléctrica de la Montaña, is an electric power cooperative serving the mountainous area, also referred to as the Cordillera Central. This region is composed of the municipalities of Adjuntas, Jayuya, Lares, Maricao, and Utuado. Like many parts of Puerto Rico, the Cordillera Central region lost power for several months as a result of Hurricane Maria in September 2017 [8]; long-lasting damage from the hurricane was compounded by the aged electrical infrastructure across Puerto Rico. Unreliable electrical service can pose challenges to affected populations, who may, for example, need to travel farther to access basic needs like food, water, and medical care. The Cooperativa Hidroeléctrica de la Montaña is currently working on an initiative to improve electrical system resilience and service reliability for customers in the Cordillera Central by designing and constructing a microgrid. These efforts include power flow modeling, to model voltages across the network and ensure that they are anticipated to stay within permissible limits, a resource assessment, to understand the solar incidence and potential solar farm placement to serve the community's needs, a resilience assessment, to understand critical service accessibility needs and impacts on community members, and a risk assessment, to characterize high-level failures and mitigation considerations.

II. Enhancing Voltage Regulation in Distribution Systems Through PV Inverter Deployment

A. Study Introduction

The increasing penetration of distributed energy resources (DERs), particularly photovoltaic (PV) systems, has introduced new challenges and opportunities in the operation and planning of electric distribution networks. Among these challenges, maintaining voltage profiles within acceptable regulatory limits is critical to ensuring power quality and system reliability. The IEEE Standard 1547 stipulates that the voltage at the point of common coupling (PCC) must remain within the range of 0.95 to 1.05 per unit (p.u.) under normal operating conditions. However, voltage deviations are increasingly observed in

distribution feeders, especially those with high resistance-to-reactance (R/X) ratios and non-uniform load distributions.

There are several research articles attempted to address the voltage regulation issue. The authors in [1] propose a coordinated voltage control strategy for improving outage quality in distribution systems with high photovoltaic (PV) penetration. It integrates control of the on-load tap changer (OLTC) at the main transformer and PV smart inverters. Using SCADA data on feeder voltages and PV output, the OLTC's tap positions are optimized daily. Meanwhile, PV inverters autonomously manage reactive power to stabilize voltage at the point of common coupling. A case study on a Taiwan Power Company substation with six feeders showed that this approach improves voltage quality and mitigates the impact of large-scale PV integration. In [2] the authors proposed a combined voltage control strategy using electronic tap changers and PV inverters. Tap changers regulate feeder voltage, while PV inverters provide local reactive power support to reduce losses. Simulations show this approach effectively maintains voltage stability and reduces losses, even with high solar variability. The research article in [3] proposes an optimal reactive power coordination strategy to manage voltage rise in feeders with high PV penetration. By using load and irradiance forecasts, it minimizes tap changer operations and prevents runaway conditions in voltage regulators. The strategy is formulated as a constrained optimization problem and shown to be effective in a distribution network model. The authors in [4] proposed a coordinated voltage regulation strategy for active distribution grids with by low X/R ratios and multiple Photovoltaic Distributed Generators. The approach utilizes an Adaptive Neuro-Fuzzy Inference System (ANFIS) to manage three voltage-based controllers: one for computing the optimal voltage reference for the On-Load Tap Changer (OLTC), another for determining Active Power Curtailment (APC) setpoints to stabilize voltage and prevent OLTC hunting, and a third auxiliary controller for reactive power adjustment to regulate voltage at the Common Coupling Point (CCP). The integrated control algorithm is implemented in MATLAB/SIMULINK and tested on a modified IEEE 33-bus distribution grid, demonstrating superior voltage regulation across all buses compared to traditional methods. In the research article [5], the authors explore the coordination of multiple voltage regulation devices—such as on-load tap changers (OLTCs), step voltage regulators (SVRs), and switched capacitor banks—in distribution networks, particularly in the presence of photovoltaic (PV) systems with smart inverters. It highlights the limitations of SVRs in maintaining voltage within acceptable limits during rapid PV output changes at sunrise and sunset. To address this, the authors propose an algorithm that coordinates SVR operations with the PV inverters' ability to curtail active power and absorb reactive power, thereby enhancing voltage regulation and power quality. The algorithm is validated using a modified IEEE-13 bus test feeder.

This study evaluates voltage regulation in Puerto Rico's distribution networks supported by the Bartolo and Adjuntas transformers. It assesses compliance with IEEE 1547 standards under different load profiles and uses a custom algorithm to identify voltage violations. To address these, PV inverters with reactive power control are deployed at critical buses. The networks are also interconnected to enhance flexibility. Simulations using a MATLAB-OpenDSS platform show that strategically placed PV inverters can effectively restore voltage levels, offering a cost-effective and adaptive alternative to traditional regulation methods.

B. PV-Inverter Control, Constraints, and Power Flow Calculation

a) A photovoltaic (PV) system consists of solar panels that convert incident solar irradiance into direct current (DC) electricity. This DC power is subsequently converted into alternating current (AC) by means of a power electronic inverter. In this study, the term smart inverter (SI) refers to a grid-connected PV inverter interfaced at the point of common coupling (PCC). The SI operates in two quadrants, enabling it to both inject and absorb reactive power based on grid requirements.

During power injection, the PV system operates with a leading power factor, exhibiting characteristics akin to a capacitive generator. Conversely, in the absorption mode, it behaves as an inductive generator, drawing reactive power from the grid and operating with a lagging power factor, as illustrated in Figure 1.

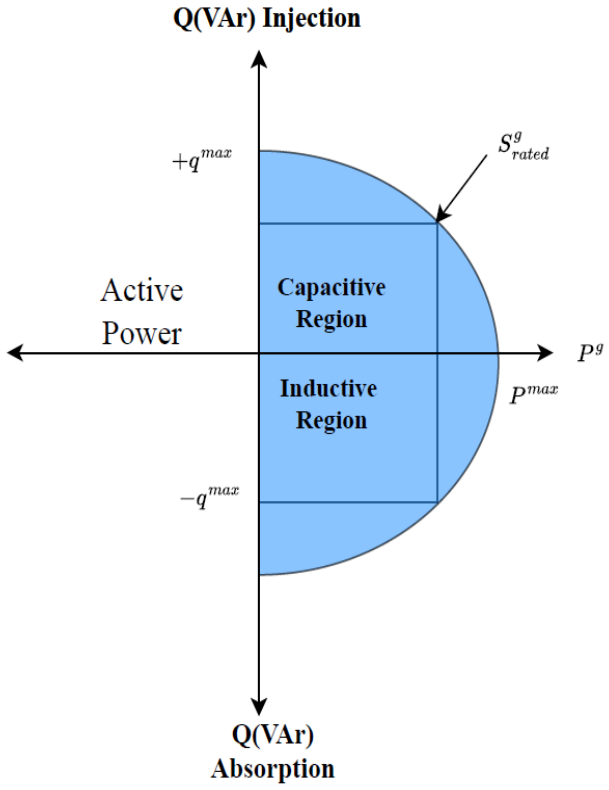

Figure 1. PV-Inverter Operation Regions [6].

The reactive power capability of the SI is constrained by its apparent power rating, which can be mathematically expressed by equation (1).

$$\sqrt{(p_i^G)^2 + (q_i^G)^2} \le s_i^G, \qquad \forall i \in \mathcal{B}^{\mathcal{G}} \tag{1}$$

In this equation, the variables p_i^G and q_i^G denote active and reactive power outputs of PV, respectively. s_i^G denotes the apparent power rating. $\mathcal{B}^{\mathcal{G}}$ represents the buses that are connected to PV, and i represents the index of the bus to which the SI is connected to. The active and reactive power output capabilities of the PV inverters are limited by the constraints shown in equation (2) and equation (3), respectively.

$$0 \le p_i^G \le p_i^{G,max}, \qquad \forall i \in \mathcal{B}^{\mathcal{G}} \tag{2}$$

$$-q_i^{G,max} \le q_i^G \le q_i^{G,max}, \qquad \forall i \in \mathcal{B}^{\mathcal{G}} \tag{3}$$

In these equations, the variable $p_i^{G,max}$ represents the maximum power of the PV-module which is proportional to solar irradiation [6].

b) The voltage regulation at the point of common coupling (PCC) is governed by the Volt-Var control function of smart inverters (SIs), which defines the reactive power output, denoted as $Q(V)$. This function, commonly referred to as the Volt-VAr curve or droop characteristic, establishes a piecewise linear relationship between the inverter's reactive power response and the local voltage magnitude, as illustrated in Figure 2.

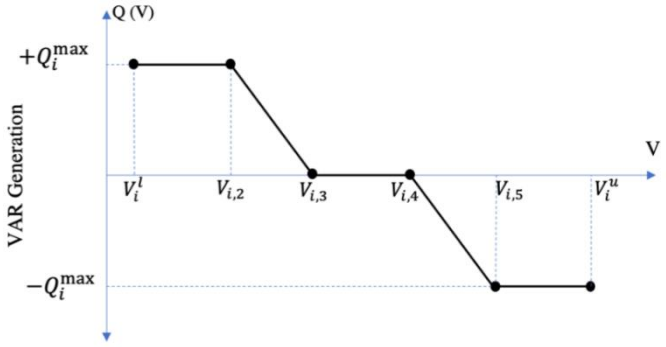

Figure 2. PV-Inverter Volt-Var Curve [6].

Within the voltage dead-band interval $[V_{i,3}, V_{i,4}]$, the inverter neither injects nor absorbs reactive power. For voltages in the range $[V_{i,2}, V_{i,3}]$, the inverter operates in a reactive power modulation mode, supplying capacitive reactive power as the voltage decreases. When the voltage drops below the interval $[V_i^l, V_{i,2}]$, the inverter reaches its capacitive saturation limit.

Conversely, in the voltage range, the inverter transitions into inductive operation, absorbing reactive power in proportion to the voltage rise. Beyond $[V_{i,4}, V_{i,5}]$, within the interval, the inverter enters the inductive saturation region. The reactive power limits and slope of each segment are defined by the inverter's control parameters and apparent power capacity. Based on that, the operating range of voltages for inverter can be mathematically expressed in equation (4) [6].

$$Q_i(V_i) \begin{cases} +Q_i^{max}, & V_i^l \le V_i \le V_{i,2} \\ \dfrac{-Q_i^{max}}{V_{i,3} - V_{i,2}} V_i + \dfrac{Q_i^{max} V_{i,3}}{V_{i,3} - V_{i,2}}, & V_{i,2} < V_i \le V_{i,3} \\ 0, & V_{i,3} < V_i \le V_{i,4} \\ \dfrac{-Q_i^{max}}{V_{i,5} - V_{i,4}} V_i + \dfrac{Q_i^{max} V_{i,4}}{V_{i,5} - V_{i,4}}, & V_{i,4} < V \le V_{i,5} \\ -Q_i^{max}, & V_{i,5} < V_i \le V_i^u \end{cases} \tag{4}$$

c) Power flow analysis equations are used to determine the steady state solution for a given set of bus loading condition as described mathematically in equation (5) for active power and equation (6) for reactive power.

$$P_{i,j} = \sum_{j=1}^{j \in N_i} |V_i||V_j|\left(G_{i,j}\cos(\theta_i - \theta_j) + B_{i,j}\sin(\theta_i - \theta_j)\right) \tag{5}$$

$$Q_{i,j} = \sum_{j=1}^{j \in N_i} |V_i||V_j|(G_{i,j}\sin(\theta_i - \theta_j) - B_{i,j}\cos(\theta_i - \theta_j)) \tag{6}$$

In these equations, the variables $G_{i,j}$ and $B_{i,j}$ denote the line conductance and susceptance of the network, respectively. The variables V_i and θ_i denote the bus voltage magnitudes and phase angles, respectively. Finally, variables $P_{i,j}$ and $Q_{i,j}$ denote the line active and reactive power flow of the network, respectively.

C. *Proposed Control Strategy*

The reactive power control algorithm governing the operation of the PV inverter is illustrated in Figure 3. This algorithm operates iteratively and is implemented through a co-simulation framework integrating MATLAB and OpenDSS. Within this framework, OpenDSS performs power flow analysis of the distribution network, while MATLAB utilizes the resulting bus voltage profiles to identify candidate nodes for PV inverter connection. The objective is to regulate bus voltages by dispatching or absorbing reactive power from the PV inverter. Specifically, if a bus voltage deviates beyond the acceptable range of 0.95 to 1.05 p.u., the algorithm initiates reactive power support from a PV inverter at that location, following the control logic defined in Figure 2. This process is

repeated iteratively until all the bus voltages are restored within the specified permissible limits.

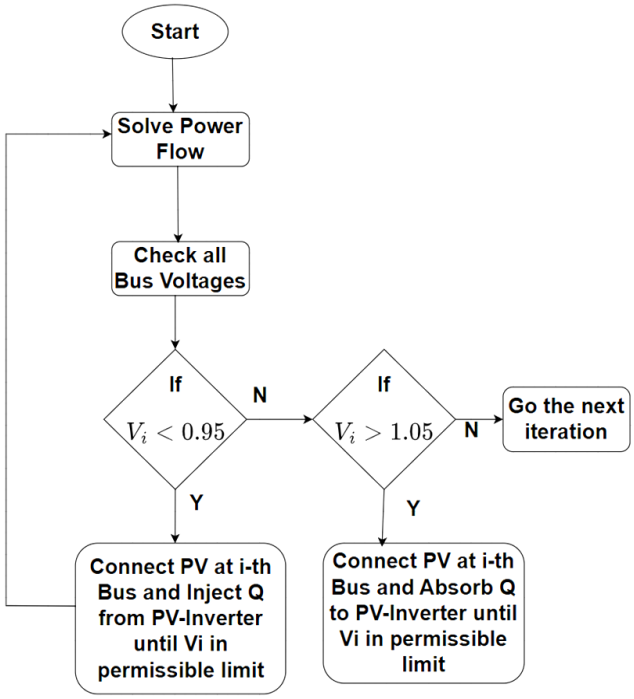

Figure 3. Flowchart of the developed algorithm.

D. Results and Discussion

This section discusses about six cases for the Bartolo and Adjuntas networks in Puerto Rico. For each case, results have displayed the voltage profiles of the networks first without PV-inverter connection, then with PV-inverter connection. The full network of Bartolo 7902 is shown in Figure 4, where the three individual feeders: 7902-01, 7902-02 and 7902-03 are shown in green, blue and red. The total load of Bartolo network is 1,144. In order to calculate the individual network load, a weighted load is considered based on the bus numbers of each network.

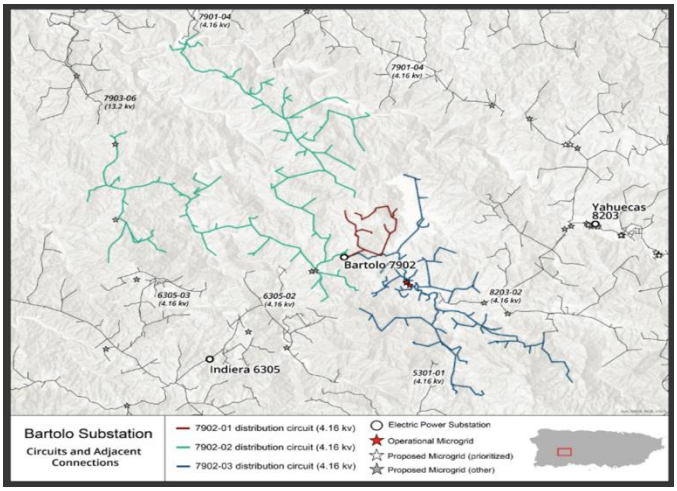

Figure 4. Bartolo 7902 Full Network.

a) Case Study 1: Bartolo 7902-01 Network

This network has 381 buses all together with 755 nodes and total load is 593 kW with a power factor (p.f.) of 0.95. This total load is then distributed among the buses using Gaussian distribution, $N(\mu, \sigma)$ where μ indicates the mean and σ denotes the standard deviation of the distribution. For this network, $\mu = 1.58$ and $\sigma = 0.5$ is considered based on the number of buses and loads. The Gaussian distribution and after that the load distribution among the buses are depicted in Figure 5 and Figure 6, respectively.

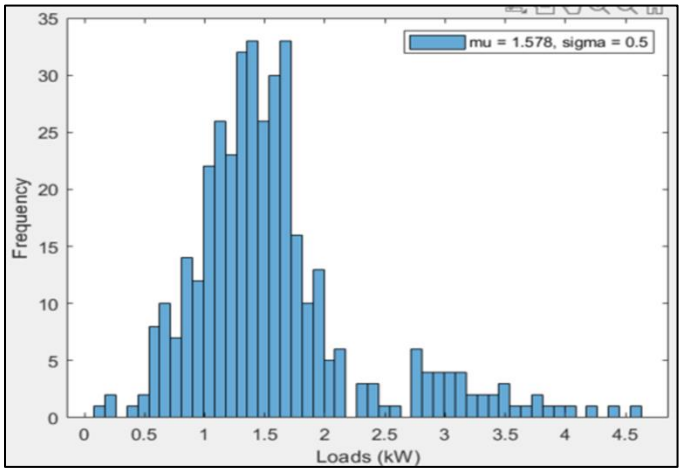

Figure 5. Gaussian Distribution of Load for Bartolo 7902-01 network.

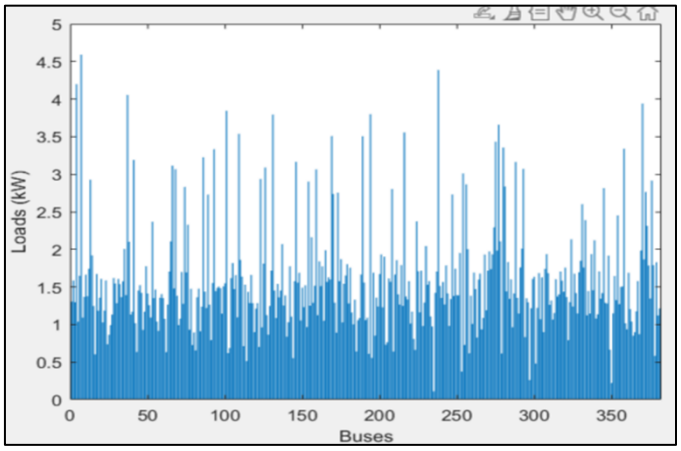

Figure 6. Load Distribution of Bartolo 7902-01 Among the Buses.

After the Gaussian distribution of loads, the per-unit (p.u.) voltage profile is illustrated in Figure 7. As it is clear in this figure, the buses farther from the distribution transformer which contain two-phases (red) and one-phase are violating the permissible limits.

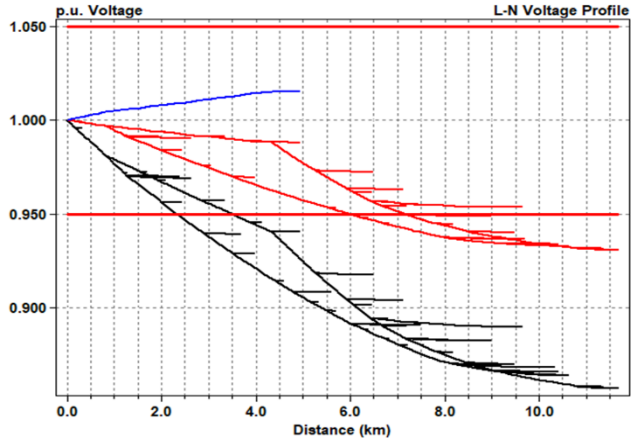

Figure 7. Voltage Profile of Bartolo 7902-01 Network Without PV-Inverter Connection

After running the proposed iterative algorithm, all the bus-voltages remain within the permissible limits of 0.5 p.u. to 1.05 p.u. as indicated by two red horizontal lines - illustrated in Figure 8.

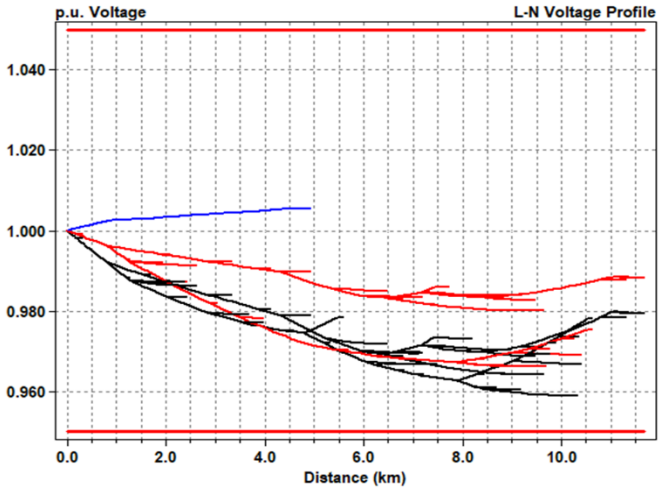

Figure 8. Voltage Profile of Bartolo 7902-01 Network After PV-Inverter Connection

b) Case Study 2: Bartolo 7902-03 Network

This network is relatively smaller comparing to the other networks of Bartolo substation. It consists of 44 buses with 100 nodes. Since the number of buses in this feeder is fewer, total load of 69 kW has been distributed uniformly among the buses. Power flow simulation is then run on OpenDSS to generate the voltage profile, which is shown in Figure 9. Since all the bus-voltages are within the permissible limits, no PV-inverters are connected to this network.

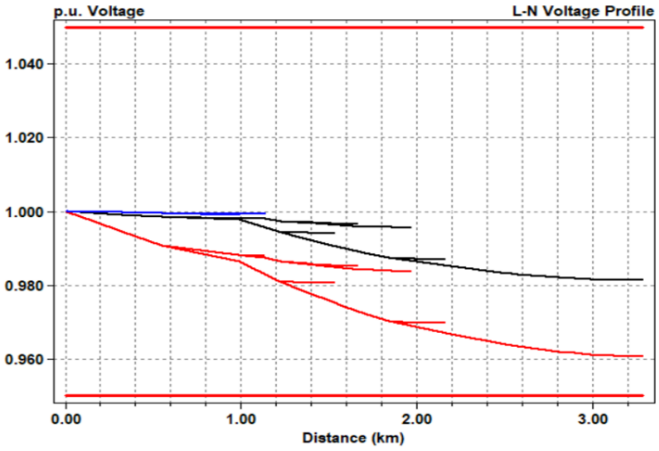

Figure 9. Voltage Profile of Bartolo 7902-02 Network Without PV-Inverter Connection

c) Case Study 3: Bartolo 7902-03 Network

This network consists total of 311 buses with 679 nodes. The total load is 484 kW for this network which has been distributed among the networks by Gaussian distribution. The mean and standard deviation of this network has been calculated as 1.56 kW and 0.5 respectively. Figure 10 shows the normal distribution where most of the loads are concentrated towards the mean value. The load distribution among the buses is shown in Figure 11. The power flow simulation is then simulated on OpenDSS, the voltage profile of which is illustrated in Figure 12. The figure shows clear voltage

violation for buses containing single phase and farther from the distribution transformer. The proposed algorithm is then run with Matlab-OpenDSS co-simulation platform which regulate all the bus-voltages of this network within the permissible limits as shown in Figure 13. The algorithm finds out two candidate buses of single phase where it connects two PV-inverters. The kVAR injection of those PV-inverters is 5.85 kVAR and 10.85 kVAR respectively. The PV-inverter rating is 100 kVA.

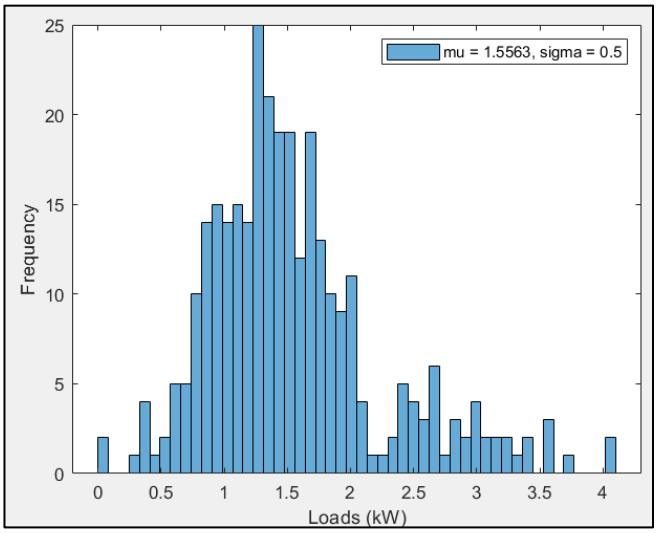

Figure 10. Gaussian Distribution of Loads of Bartolo 7902-03 Network

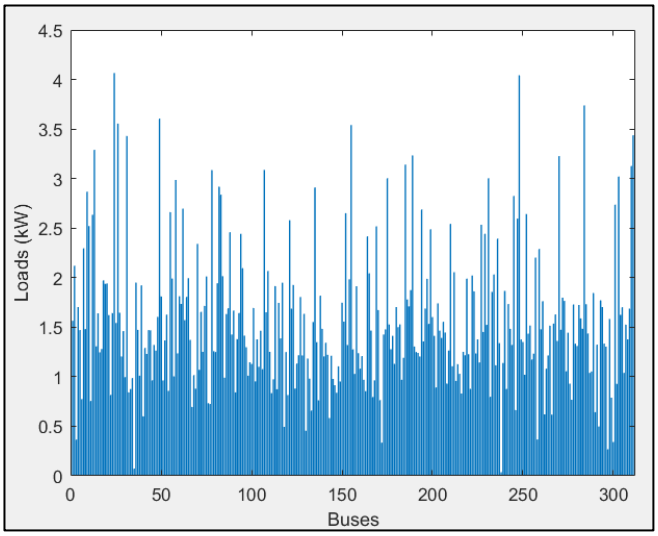

Figure 11. Load Distribution Among the Buses of Bartolo 7902-03 Network

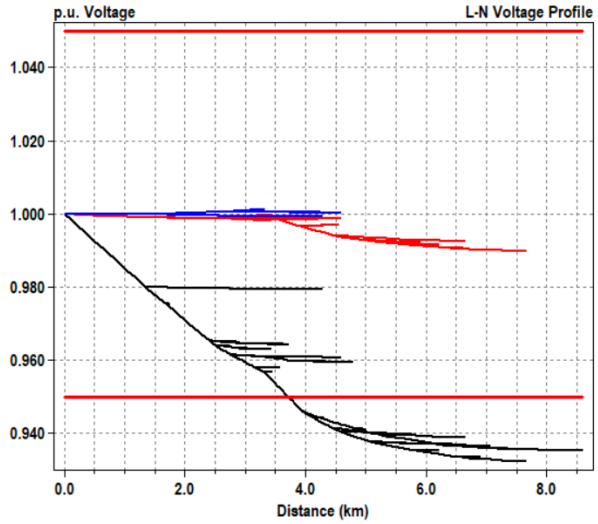

Figure 12. Voltage Profile of Bartolo 7902-03 Network Without PV-Inverter Connection

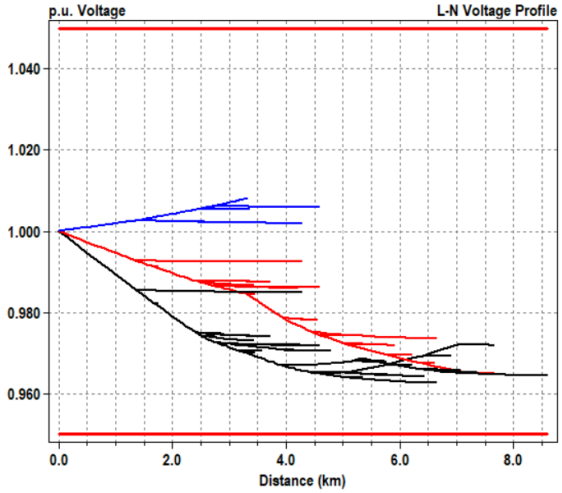

Figure 13. Voltage Profile of Bartolo 7902-03 Network with PV-Inverter Connection

d) Case Study 4: Adjuntas 8203-02 Network

Adjuntas substation transformer has a total capacity of 1548 kW and total number of 953 buses, whereas 8203-02 feeder branches to 387 buses with 816 nodes. So the weighted load of 630 kW has been distributed normally as shown in Figure 14 with mean=1.63 and standard deviation=0.5. The load distribution among the buses is illustrated in Figure 15.

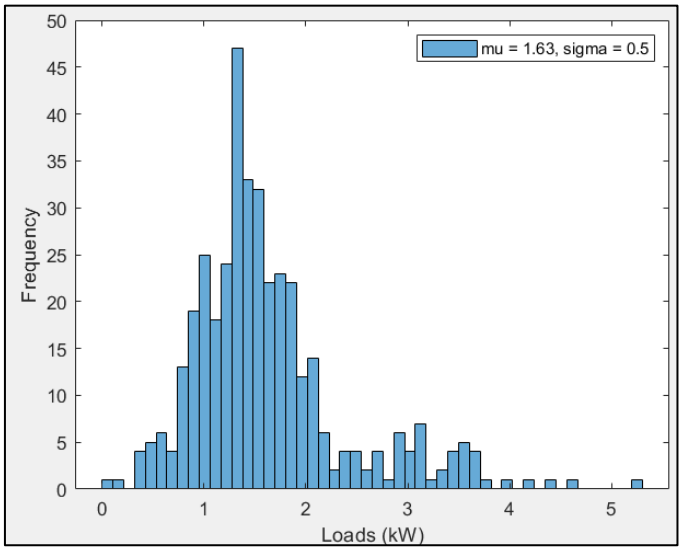

Figure 14. Gaussian Distribution of Loads of Adjuntas 8203-02 Network.

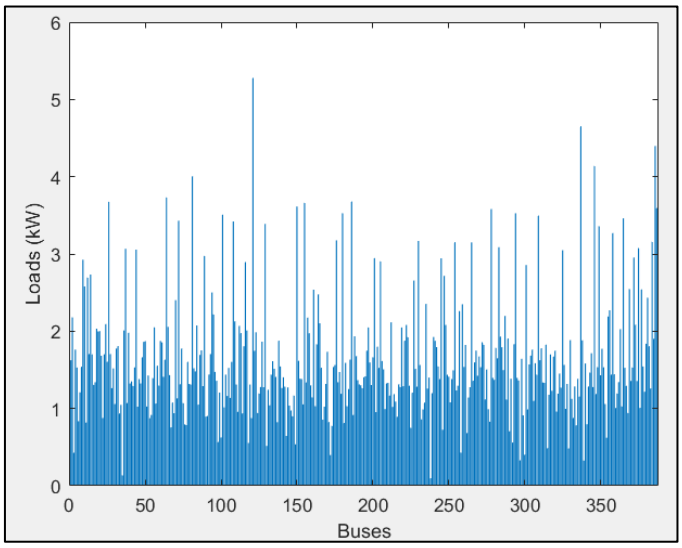

Figure 15. Load Distribution Among the Buses of Adjuntas 8203-02 Network

As illustrated in Figure 16, voltage violations are observed primarily at buses that are single-phase (indicated in black) and located farther from the distribution transformer. Since the majority of bus voltages remain within the acceptable limits, the algorithm identifies that only a limited number of PV inverters are required, each with minimal reactive power support. Specifically, the algorithm selects two PV inverters, each rated at 100 kW, dispatching 6 kVAR and 11 kVAR of reactive power, respectively. The resulting voltage profile, shown in Figure 17 confirms the effectiveness of the proposed algorithm.

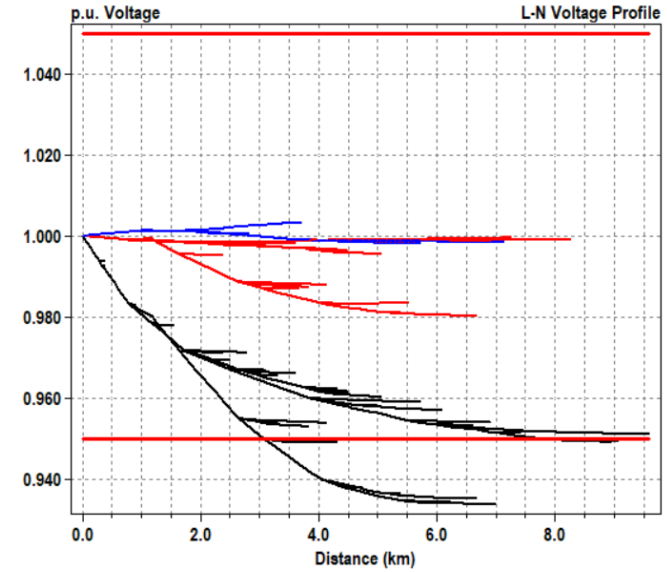

Figure 16. Voltage Profile of Adjuntas 8203-02 Network Without PV-Inverter Connection

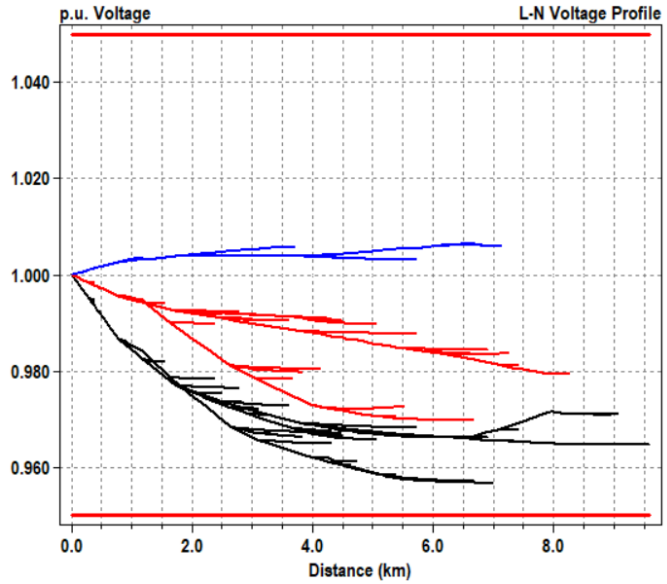

Figure 17. Voltage Profile of Adjuntas 8203-02 Network With PV-Inverter Connection

e) Case Study 5: Bartolo-Adjuntas Interconnection

This case study investigates the interconnection of the Bartolo 7902-03 and Adjuntas 8203-02 distribution networks via a 15.2-meter three-phase distribution line. The objective is to evaluate whether either the Bartolo or Adjuntas transformer can independently sustain the entire load of the combined network in the event of a transformer outage. This analysis assumes necessary upgrades to transformer capacity and the three-phase interconnection point to accommodate the increased load demand. Figure 18 shows the interconnection point of these two networks by a black circle. The total load of this network after the connection is 1155 kW, with total 697 total buses and 1492 nodes. Loads are distributed normally as

previous cases, and the Gaussian distribution of loads is illustrated in Figure 19. The spatial distribution of loads across the buses is presented in Figure 20. Upon applying the nominal load distribution, a power flow analysis was conducted, with the resulting voltage profile shown in Figure 21. Significant voltage violations are observed, particularly at single-phase buses (highlighted in black), along with some two-phase buses (shown in red). Notably, several single-phase buses located farther from the distribution transformer exhibit voltage levels below 0.8 p.u., indicating a need for substantial reactive power support from PV inverters. That is exactly the algorithm determines: The control algorithm identifies and connects six single-phase PV inverters, each rated at 100 kVA with a maximum reactive power support of 98 kVAR, to mitigate voltage violations. Additionally, one two-phase PV inverter providing 7.5 kVAR of reactive support is deployed to further enhance voltage levels within acceptable limits. The effectiveness of this reactive power compensation strategy is demonstrated in Figure , where the voltage profile shows significant improvement across the network.

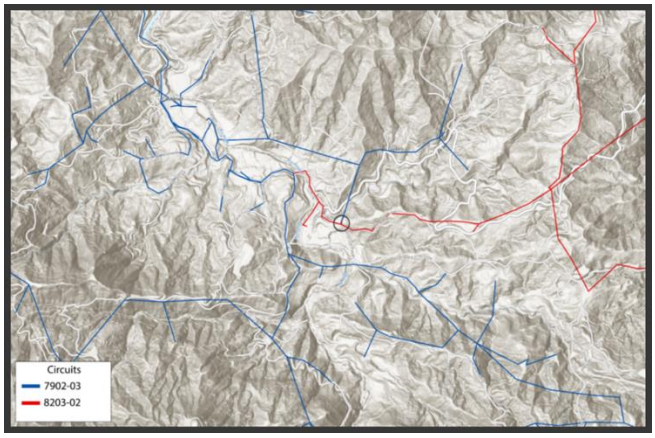

Figure 18. Bartolo-Adjuntas Connection Point

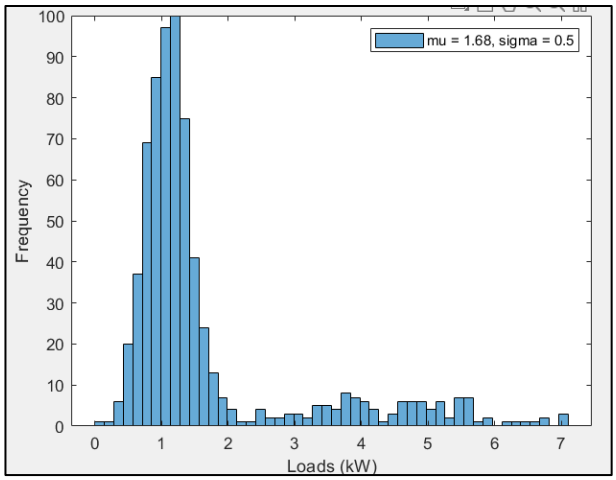

Figure 19. Gaussian Distribution of Loads of Bartolo (7902-03) and Adjuntas (8203-02) Network

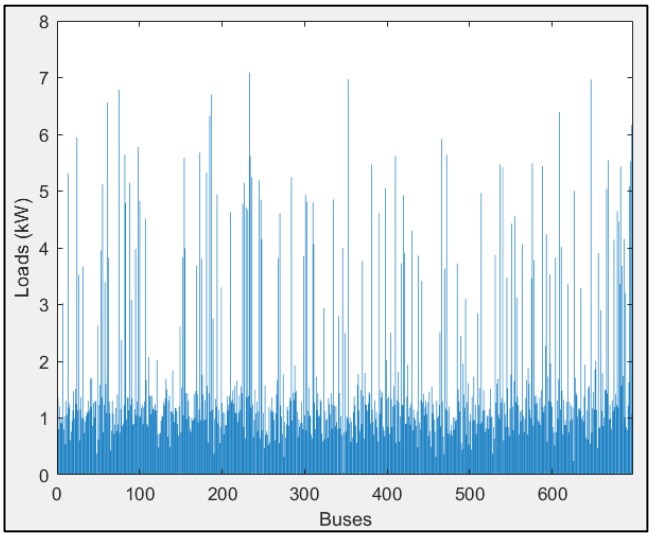

Figure 20. Load Distribution Among the Buses of Bartolo (7902-03) and Adjuntas (8203-02) Network

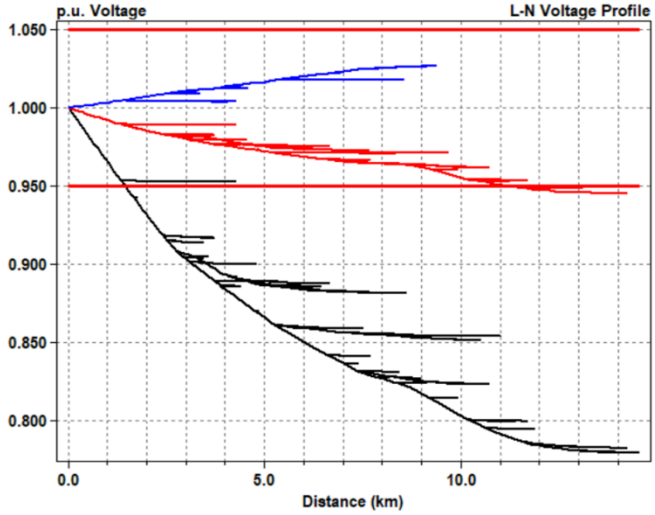

Figure 21. Voltage Profile After Bartolo-Adjuntas Connection Without PV-Inverter Connection

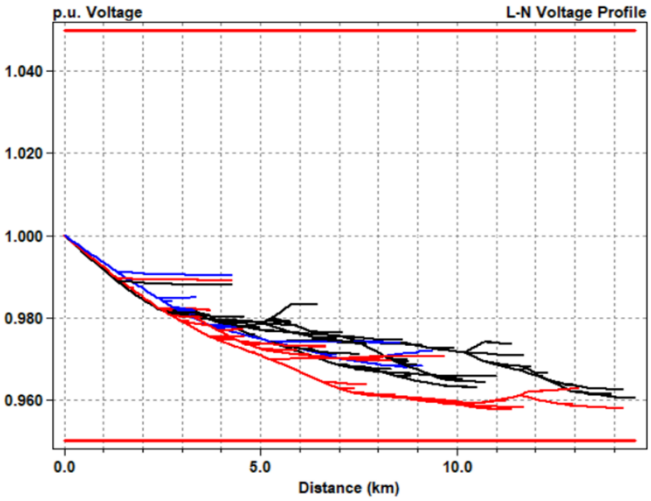

Figure *22*. Voltage Profile After Bartolo-Adjuntas Connection with PV-Inverters

E. Overall Findings

The findings from the steady-state analysis clearly demonstrate that integrating PV inverters into the distribution network provides an effective and economically viable solution for voltage regulation, even in an unbalanced distribution system usually characterized by high resistance-to-reactance (R/X) ratios. Compared to conventional methods such as transformer tap-changing and capacitor bank installations—which often involve higher capital and operational costs—PV-based reactive power support offers a flexible and scalable alternative. Moreover, the proposed control strategy contributes to the enhanced operational lifetime of OLTC-equipped transformers by significantly minimizing the frequency of tap changes, thereby reducing mechanical wear and extending the transformer's service life. Future research will focus on enhancing the iterative PV-hosting capacity algorithm by incorporating multi-objective optimization techniques. These enhancements will introduce additional constraints aimed at minimizing active power losses and minimizing reactive power injection/absorption while further improving voltage profiles toward the nominal 1.0 p.u.

III. Conceptual Substation Microgrid Analysis

Conceptual substation microgrid analysis was conducted using Sandia National Laboratories' Microgrid Design Toolkit (MDT). MDT is an early-stage decision support software that can provide microgrid design tradeoffs for a variety of possible microgrid solutions. MDT allows the user to apply objectives for performance, reliability, and cost to compare alternative microgrid designs.

The MDT is a resilience-based design tool and requires the following inputs: 1) Electric Load Demands, 2) Generation/Storage Assets (including output profiles for intermittent generation assets such as solar, wind, and hydropower), 3) Design Basis Threats (DBT) resulting in utility outages, and 4) Optimization Parameters. Components can be made fixed or given a variety of design alternatives to evaluate, which can easily result in the thousands of possible combinations in the solution space, sometimes much more.

In this study, the search space was set to evaluate tradeoffs between the purchase cost and the energy availability performance metric. Energy availability is defined as the percentage of the total load energy (kilowatt-hour [kWh]) that was delivered by each design across all DBTs simulated. Multiple solutions are simulated based on the simulation length chosen, which can be set to the number of years desired to simulate utility outages and the coincidence between load and the availability of energy generation resources (e.g., solar irradiance for solar energy generation). Potential solutions are produced with performance statistics, providing a variety of solutions to compare.

Assets that were provided for consideration in the simulations were solar PV and battery energy storage system (BESS). Hourly, site-specific PV production profile estimates were developed for the simulations. Purchase cost estimates for PV and batteries were developed and implemented in the equipment specifications for each, which were then set as design options. These costs are upfront purchase cost estimates for comparison. In this study no failure modes (periodic component failures) were implemented, which means all results assume the assets were always functional.

The MDT results for the simulations include the purchase cost and energy availability for each design. Some PV spatial perspectives were also formulated.

A. Substation Load Demand Profile Development

In alignment with the OpenDSS analysis, it was desired to simulate the Bartolo Substation in MDT as well. Power flow analyses, as are performed in OpenDSS, are commonly done using a snapshot of load demand, such as the peak load. In MDT, it is more ideal to using longer term temporal profiles, such as annual hourly demand (8,760 hours), which can simulate diurnal and seasonal variations and the needs to serve the loads during many different coincidences between load and PV, both hourly and over the course of long outages.

While it was possible to use what seemed to be valid Bartolo Substation load demand snapshots for the OpenDSS studies, the available annual data profiles for the Bartolo Substation were very poor quality. It is sometimes feasible to scrub load demand profiles, mending and removing data dropouts or obviously unrealistic outliers, in this case, the data was too severely flawed to modify into an ideal, baseline substation demand profile.

This led to the search for the next best match amongst the other substations, and fortunately, the next nearest substation, Indiera Substation, had a good quality annual profile for 2019. Adding to the ideality of using Indiera Substation load data for a Bartolo Substation study was the similarity in substation transformer ratings; 1,144 kVA for Bartolo Substation and 836 kVA for Indiera Substation. Also, this was supported by the similarity in observable annual peak demands; 660 kVA for Bartolo Substation and 700 kVA for Indiera Substation. Figure 23 shows the 2019 Indiera Substation load demand profile in kilowatts, assuming a 0.95 power factor conversion from the apparent power units (kVA) referenced. This profile was used for all Bartolo Substation simulations.

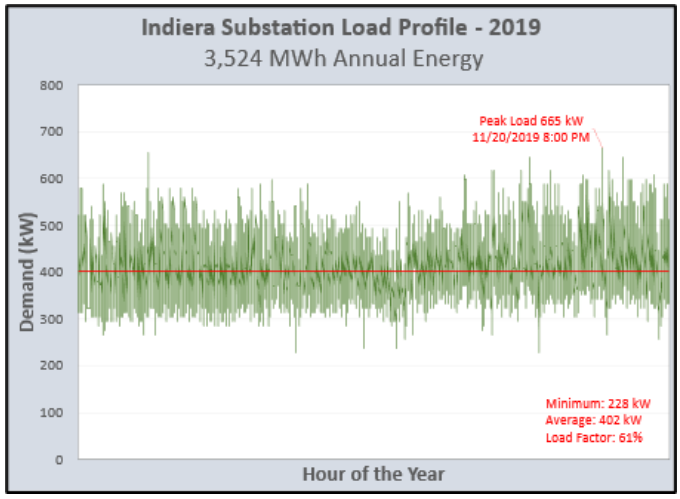

Figure 23. Indiera Substation 2019 Load Demand Profile, Hourly Data

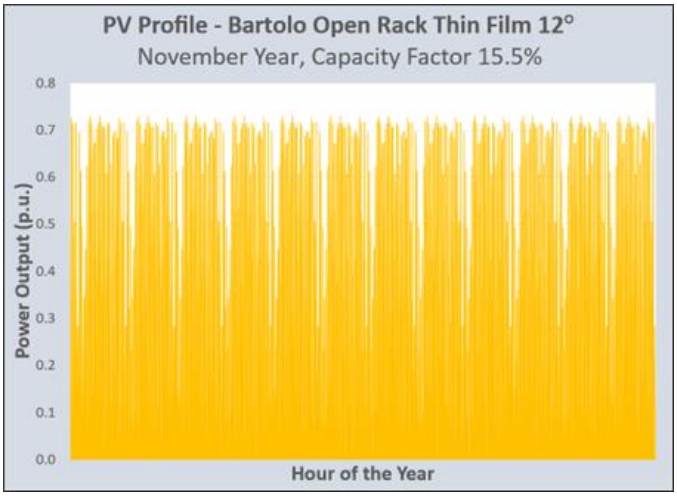

Figure 24. Bartolo Substation MDT Study PV Profile, 12-degree Tilt, PVWatts November Duplicated [7].

B. PV Power Output Profile Estimation

To simulate PV power output in MDT, it is necessary to upload resource profiles for each. Several options are available for the timespan and resolution of uploaded resource profiles. Resource profiles are entered in per unit values, which are then scaled by the nominal power rating of the options created and chosen in a model.

For this study, and annual-hourly resource profile for PV was used, which was derived from the National Renewable Energy Laboratory's (NREL) PVWatts Calculator [7]. The Bartolo Substation area has many National Solar Radiation Database (NSRDB) weather data areas to choose from, which the PVWatts tool then uses to calculate a PV power output estimate, along with several other input options. The other most important input setting was the assumption that the PV systems would be installed with a 12-degree tilt to the south, per the recommendation of the project team as a previously determined optimum tilt for production and wind resistance.

Due to the resulting PVWatts profile derived from the generalized NSRDB weather data areas and the typical meteorological year processing of historical data, it was determined by the project team that most of the PVWatts monthly solar radiation averages (kilowatt-hours per meter squared per day [kWh/m^2/day]) were higher than historically expected in specific areas of the Bartolo substation service area. Therefore, the lowest solar radiation average month (November), with an average solar radiation of 4.85 kWh/m2/day, was chosen to be repeated for the annual PV profile. The PV profile used in the Bartolo Substation analysis is shown in Figure 24.

C. PV and BESS Purchase Cost Estimates

Cost minimization, which is essentially a default optimization metric in MDT studies, was incorporated in the MDT optimization metrics for the Bartolo Substation analysis. To incorporate cost minimization, it is necessary to provide purchase cost estimates for all options in the MDT model. All options must be defined in their respective equipment specification sections, where they are all given a unique name, capacity ratings, costs, and several other details that are available. For this study, cost rates for PV and BESS were used to designate purchase costs to all options for each.

For the basis of the PV cost rate, NREL's 2024 Annual Technology Baseline (ATB) was referenced, specifically the 2026 conservative capex estimate for commercial PV. A 66% increase was implemented internally for potentially anticipated increases to the mountain regions of Puerto Rico.

For the BESS cost estimates, the Tesla Megapack purchase site was referenced. The Tesla Megapack pricing was not chosen as a recommendation, but rather because it makes its pricing publicly available and offers the selection of pricing for Puerto Rico. While BESS pricing is dependent on both the charge/discharge rating (kW) and the energy storage rating (kWh), for simplicity, the MDT analysis applied a cost rate for the storage rating (kWh) only, which is around 75% of the total cost for Tesla Megapacks. Again, a 66% increase was applied to the quoted purchase cost, but in this case not just for the potential regional cost increases, but also because the Tesla Megapack purchase cost does not include other capex aspects that are included in the NREL ATB PV estimates, such as interconnection costs, balance-of-system costs, and others. Table 1 lists the PV and BESS purchase cost rates used.

TABLE 1.
PURCHASE COST ASSUMPTIONS FOR PV AND BESS USED IN MDT ANALYSIS

Asset Type	Power Rate ($/kW)	Energy Rate ($/kWh)	Source
PV	3000	N/A	2024 NREL ATB4 plus 66%
BESS	N/A	480	Tesla Megapack5 plus 66%

D. Design-Basis Threats

The MDT is intended to be an islanded microgrid design tool, which means it requires islanding events, i.e. grid outages, to design against. DBTs are the method by which utility outages are defined, which can include multiple separate entries if desired. The performance statistics for each solution produced are in reference to the performance across all DBTs simulated. DBTs are defined primarily with two aspects, frequency of occurrence and duration. Both aspects are entered in units of hours and can be defined with a variety of probability distributions available to be applied to either aspect, if desired. While there is extensive historical outage information from which to draw upon for the area, as well as Puerto Rico as a whole, for this study a single DBT entry of 30-days duration and occurring approximately once a year (exponential distribution) was used. A simulation length of 130 years results in approximately 120 outages simulated per solution, where the intention was to have approximately 10 outages simulated each month of the year. The simulation length is not to suggest the expectation of the life of the microgrid, but rather to allow the simulation to go through a thorough set of outage simulations, virtually covering all 30-day outage windows throughout the year between the PV output and the load demand. Being 30-day outages with just PV and BESS options, it can be argued that these solutions would support the substation area for the entire year at the performance levels reported.

E. Bartolo Substation MDT Analysis

An MDT analysis was conducted for the Bartolo Substation with PV and BESS options only. Solar options from 3 to 24 MW (1 MW increments) and BESS options 4 to 80 MWh (1 MWh increments, with a conservatively sufficient power rating for charging/discharging) were selected for the optimization.

Performance metrics of cost minimization and load energy availability maximization were used for the optimization. Energy availability is reported as a percentage in the results and indicates the percentage of the load energy supplied (kWh) during all simulated outages for each solution.

The Bartolo Substation MDT simulation produced 32 different solutions, all with tradeoffs between cost and energy availability. The results can be plotted simply in a Pareto frontier, which simply plots a point for each solution on the axes of the performance metrics set, in this case cost and energy availability. To provide context of the upper bookend of the solution set, e.g. the 100% energy availability solution, Figure 25 shows the associated MDT solution diagram with details added.

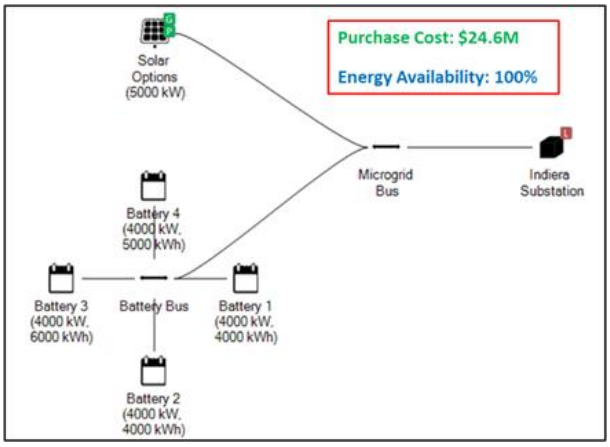

Figure 25. Bartolo Substation 100% Energy Availability Solution Diagram

Figure 26 shows the Pareto frontier of solutions, with the energy availability on the x-axis and purchase cost on the y-axis. Formatted in this way, the exponential nature of cost as the solutions approach 100% energy availability can be seen, which is a common observation amongst similar studies. This can be due to the coincidence between load demand and PV output, where a baseline of coincidence between the two can be expected, but also an increasingly difficult to serve set of outliers that increase the cost disproportionately with respect to the energy availability.

One of the benefits of the Pareto frontier plot is the ability to observe the "knee" area of the solutions, where the largest tradeoffs between energy availability increases for the smallest cost increases nearing the performance targets can be analyzed. These usually precede the area of solutions with steep cost increases for relatively small energy availability increases, nearing 100%. Figure 27 highlights the optimal solutions (denoted in green in Figure 26) in a column plot that includes purchase cost (x-axis), PV power rating (yellow columns), BESS energy rating (brown columns), and energy availability percentage (blue line with markers).

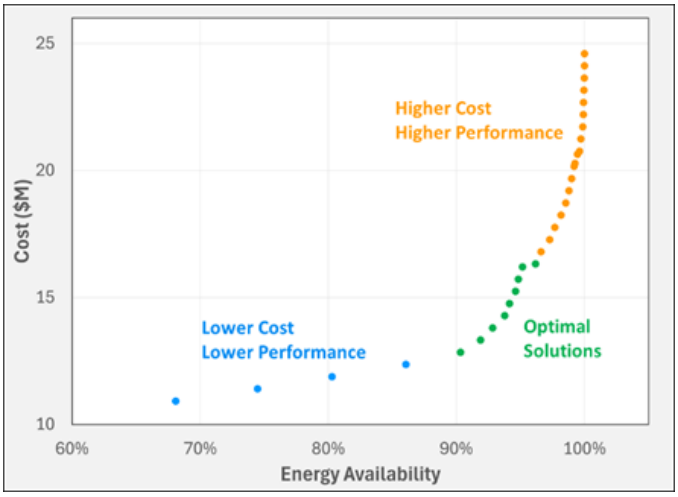

Figure 26. Bartolo Substation MDT Simulation Pareto Frontier of Solutions.

Figure 28 is identical in format to Figure 27, but for the four lower cost, lower performance solutions (denoted in blue in Figure 26).

Referencing the 100% energy availability solution shown in Figure 25, and assuming 5 acres per MW for PV, this would require 25 acres of land for the 5 MW PV system. For initial reference, Figure 29 shows a satellite image of the Bartolo Substation feeder topologies and service transformer locations (denoted with small white circles), with an estimated 744 customers. Figure 30 then shows the Bartolo Substation service area with an orange rectangle showing the relative size of 25 acres in the area, which would theoretically be sufficient to host the upper bookend of 5 MW of PV to serve the substation microgrid at 100% energy availability. Finally, Figure 31 shows a zoomed view of the 25-acre area shown in Figure 30.

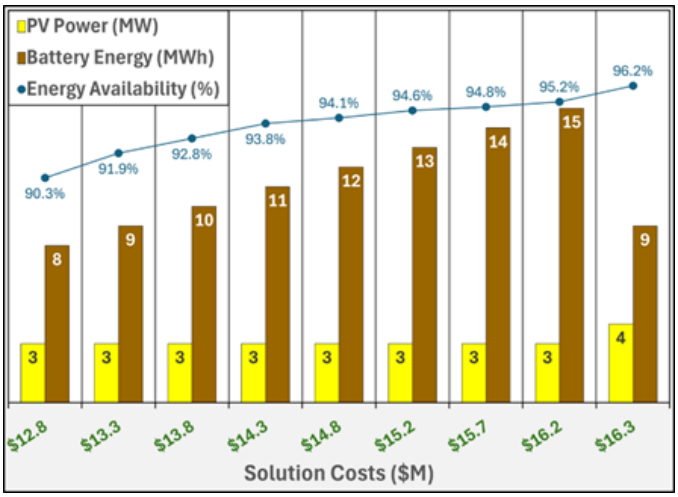

Figure 27. Bartolo Substation Optimal MDT Solutions Column Plot

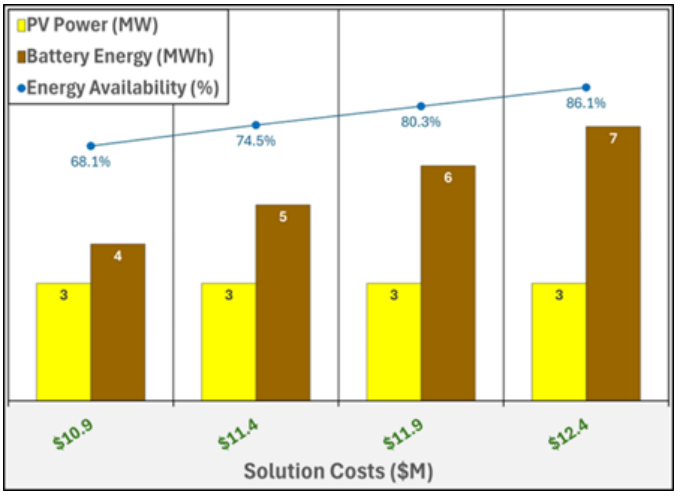

Figure 28. Bartolo Substation Lower Cost, Lower Performance MDT Solutions Column Plot

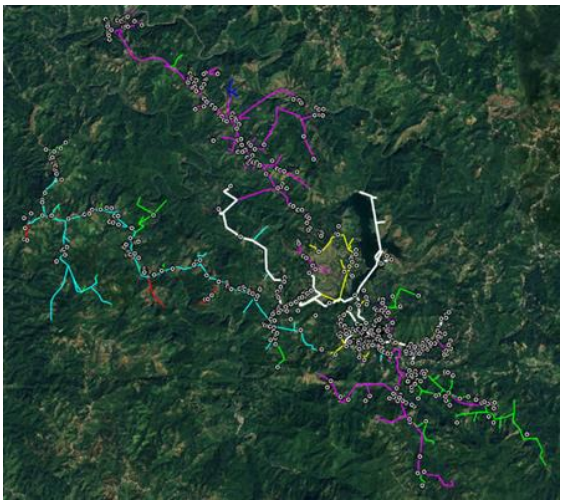

Figure 29. Bartolo Substation Service Area (~744 Customers)

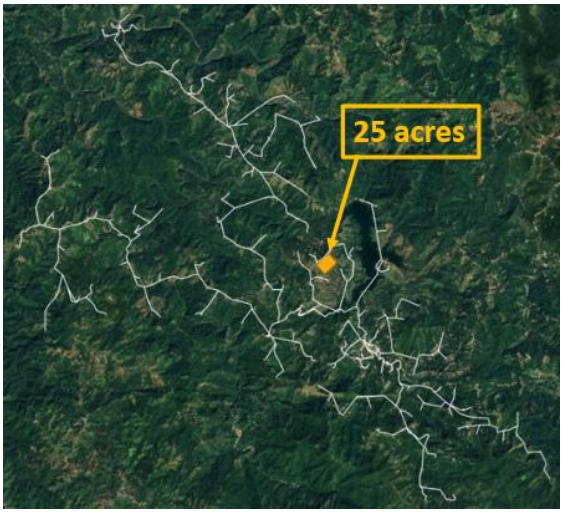

Figure 30. Bartolo Substation Service Area with 25-Acre Rectangle Example Relative to Area

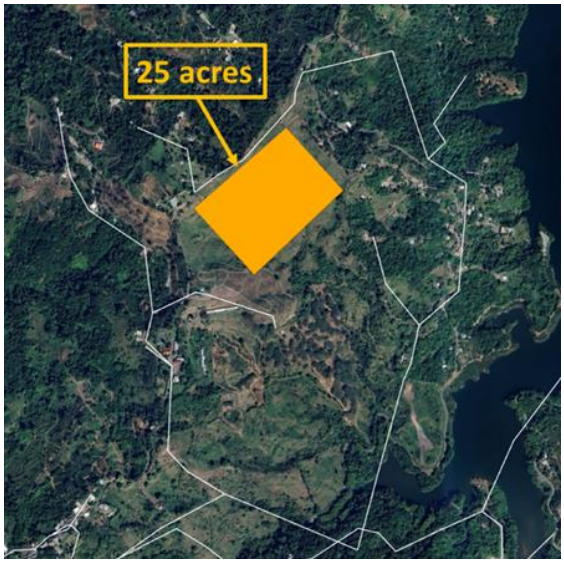

Figure 31. Bartolo Substation Area Zoomed-in View of 25-Acre Area.

Note that the microgrid analyses are very dependent on the assumed coincidences between various temporal aspects, such as PV output and load demand in this case. Even when historical, measured, time-synchronized data is available and used for simulations, it can still be expected that coincidences will vary year-to-year with weather and other factors. It is therefore difficult to recommend the best energy availability target from the solutions and further, more detailed studies would be necessary. These are meant to give a preliminary idea of what it would take to serve the assumed load demand.

While serving the Bartolo Substation area at a lower energy availability, such as those highlighted in Figure 27 and Figure 28 would result in the potential reduction of land/rooftop needed for PV, as well as purchase cost, there are other considerations. To feasibly realize lower energy availability solutions, it would be likely that some level of load controls and communications would be needed, e.g., for instances where load demand exceeds generation/storage resources, to avoid system destabilization. Such capabilities would likely have non-negligible cost and management aspects. This study did not include any potential economic benefits whether they to be connected to the grid for any period.

Another study aspect that would require additional analysis would be the ability for the systems to handle sub-hourly transients, such as motor startup currents, etc. This microgrid study, using averaged hourly data, arguably addresses the substation load energy needs to some accuracy, but not to more detailed stability power flow aspects. Depending on the final location of any new assets, such as PV and BESS anywhere other than at the existing substation location, it would also be necessary to assess the need for potential system protection evaluations and upgrades as well.

IV. Microgrid Resilience Assessment

Many factors and priorities must be considered when designing and operating a microgrid, such as energy generation assets and resources, loads, geographical connectivity, existing infrastructure, and economic viability. In addition, having a holistic understanding of the economic, time, and other challenges faced by people attempting to access critical services can be helpful for decision-making [8]. These critical services can include facilities such as utilities (e.g., water, electricity), grocery stores or supermarkets, medical care centers (e.g., hospitals, clinics), and community centers. The purpose of this study was to propose specific microgrid connections to loads and energy generation asset numbers based on a balance between improved accessibility to energy-dependent critical services and the cost of constructing a microgrid to keep these facilities powered during a main grid outage or other disturbance.

A. Model Development

We used Feeder 7902, which is the feeder line supported by the Bartolo distribution transformer, for the case study. This feeder is located primarily in the municipalities of Lares and Adjuntas, with some small sections of the feeder crossing the county borders into Las Marías, Maricao, and Yauco. The feeder is comprised of 3 distinct networks, referred to as 7902-01, 7902-02, and 7902-03; however, the feeder resilience study was conducted for the overall 7902 network.

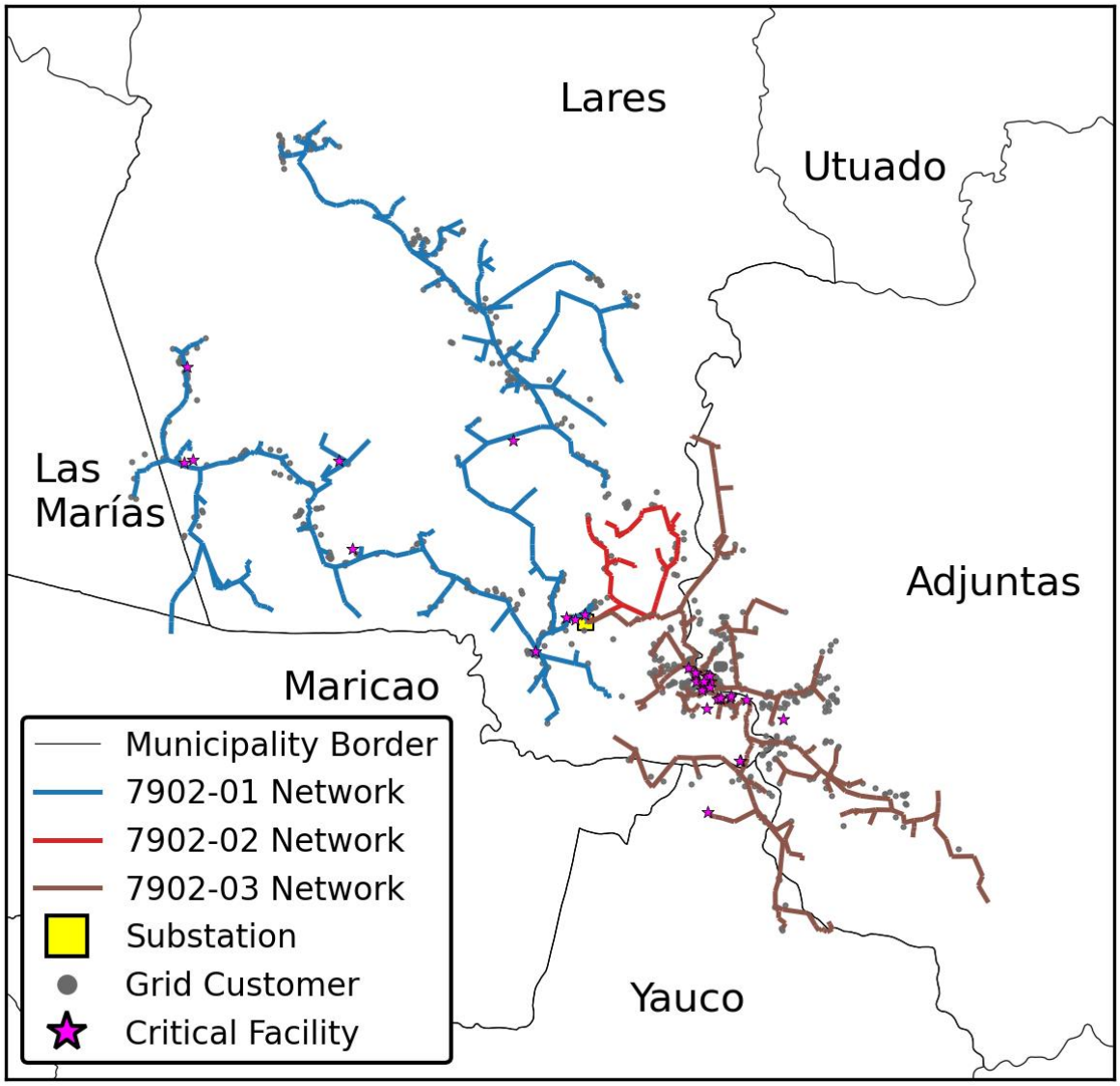

Figure 32. Bartolo Feeder by Network Showing Load Locations (Critical Facilities and Other Grid Customers)

The Resilience Node Cluster Analysis (ReNCAT) tool was used for this study. The main principle of the tool is to find options for investments in microgrid components such as switches on an existing feeder and energy generation assets, with the different options focusing on their cost and impact on the population being served [8]. The ReNCAT analysis finds solutions for which switches to use to power and un-power sections and loads along the feeder to reduce both cost and burden. Increasing the resilience of the feeder by developing microgrids decreases the additional effort that people may need to exert to continue accessing critical facilities during times when there is a power outage of the main grid. This parameter describing the effort and resources needed, and challenges faced, when accessing critical services, is a main metric calculated by ReNCAT. Improving local electrical infrastructure also increases costs, however, so the two key considerations of this ReNCAT metric and cost must be accounted for in a resilience analysis.

Data were collected and assumptions were made for various related inputs for the critical and noncritical loads within the electrical system, including electricity usage and costs.

B. Load Characteristics

First, we identified critical loads in the area of each feeder network by cross-referencing and creating a combined list from a critical loads list provided to Sandia National Laboratories by the Puerto Rico utility LUMA, a separate list of critical loads compiled previously by Sandia National Laboratories [8], a list of planned emergency locations provided by the Cooperativa Hidroeléctrica de la Montaña, and looking at Google Maps. We divided critical loads into the following categories: cell towers [9], official and unofficial emergency muster points, grocery

stores, restaurants, gas stations, medical treatment centers, farms, and water treatment facilities.

We then estimated the energy usage of these critical services using the approximate area of each critical service, measured from Google satellite images, and published values for national median source energy use intensity (EUI) for different facility types [10]

TABLE 2.
CRITICAL LOAD DATA

Facility Category	Facility Name	Latitude	Longitude	Estimated Area (ft^2)	EUI (kBtu/ ft^2)	Calculated or Assumed Total Load (kW)
Cell Tower	Cell Tower 1	18.18173	-66.8332	-	-	10
	Cell Tower 2	18.18102	-66.834	-	-	10
	Cell Tower 3	18.18032	-66.8332	-	-	10
	Cell Tower 4	18.17897	-66.8319	-	-	10
Emergency Muster Point	Centro de Apoyo Mutuo Bartolo	18.18928	-66.8494	1593.16	109.6	5.84
	Capilla Virgen de la Medalla Milagrosa	18.18867	-66.8507	1049.59	58.4	2.05
	Iglesia Episcopal Mision San Bartolome Apostol	18.18889	-66.8517	1050.12	58.4	2.05
	Iglesia de los Hermanos en Jesucristo	18.208	-66.9013	3081.56	58.4	6.02
	Iglesia del Senor de Uncion, Poder y Fuego	18.17634	-66.8237	3606.77	58.4	7.05
	Lisandra Church	18.18263	-66.8359	2555.02	58.4	4.99
	Parroquia Nuestra Senora de la Medalla Milagrosa	18.18192	-66.835	6786.01	58.4	13.26
	Seventh Day Adventist Church - Castaner	18.17994	-66.8342	2177.62	58.4	4.25
	Mision La Santa Cruz	18.17887	-66.8318	2561.57	58.4	5
	Iglesia Bautista de Castaner	18.17874	-66.8284	8205.44	58.4	16.03
	Policia de Puerto Rico – Precinto Castañer	18.17881	-66.8322	836.43	124.9	3.5
	Estación de Bomberos de Castañer	18.18098	-66.8349	2084.96	124.9	8.71
	Escuela Superior Gabriela Mistral	18.17924	-66.8305	3669.82	104.4	12.82
	Escuela Julio Lebron Soto	18.18163	-66.8336	3778.72	104.4	13.2
	Centro Comunal de Castaner	18.17763	-66.8335	5906.83	109.6	21.66
Grocery Store / Supermarket	Here I Stay	18.20822	-66.8813	3114.48	444	46.26
	The Tower Juices	18.20837	-66.9002	-	-	46.26
	Supermercado Mega Fresh Castañer	18.17895	-66.8306	5645	444	83.85
Restaurant	Castaner Bakery	18.18082	-66.834	2059.66	527.7	36.36
	La Profe's NutriStop & Go	18.18203	-66.8351	1062.41	573.7	20.39
Gas Station	Gasoline Garage	18.21071	-66.8587	1020.18	883.5	30.15
	Colmado y Gasolinera Serrano	18.18469	-66.8558	-	-	30.15
Medical Treatment Center	Lares Medical Center	18.19739	-66.8796	7404.55	145.8	36.12
	Hospital General Castañer	18.18097	-66.833	36540	426.9	521.87
Farm	Hacienda Asunción	18.16487	-66.8335	-	-	10
Water Treatment Facility	Tanque Alemañy	18.21982	-66.901	86.7	5.9	0.02

Next, we used 1,144 kW as the total load for all networks in the 7902 feeder, based on the OpenDSS model for Bartolo, Using a proprietary dataset from LUMA for electricity customer locations across Puerto Rico, we determined how many non-critical electricity customers (e.g., residential customers or non-critical facilities) were on the entire feeder, assuming no overlap between this customer list and the critical loads we identified previously. In other words, all customers included in this dataset were assumed to represent noncritical loads. We then subtracted the power consumption of all critical loads on the feeder from the total network load and divided by the number of customers on the feeder to estimate the load per customer.

For the critical loads, we considered that all critical loads are eligible for disconnection from the power line to which they are connected, in the event that a power outage on the main grid occurs and the power line to which they are connected is drawing power from the microgrid generation assets only. Based on satellite images and knowledge of the critical loads in the list, such as the Hospital General Castañer, many of these facilities already have backup generation for emergencies. These generation assets often include solar panels and/or diesel generators.

C. Critical Load Service Mapping

The ReNCAT model also requires a characterization of the critical loads in terms of the services they provide, including shelter, communications, food, fuel, safety, water, and medication. We used the following classifications for this analysis, across all feeders.

TABLE 3.
SERVICE CLASSIFICATIONS FOR CRITICAL LOADS

	Shelter	Comms.	Food	Fuel	Safety	Water	Meds.
Cell Tower		5					
Emergency Muster Point	5	4			5	2	2
Grocery Store			5			5	3
Restaurant			5			4	
Gas Station			4	5		4	
Medical Treatment Center	4				5		
Farm			5				
Water Treatment Facility						5	

We assigned a mapping number of 5 for services at facilities whose main purpose is to provide those services, and lower numbers for ancillary services. Gas stations were given a rating of 5 for fuel and 4 for both food and water, since many gas stations have convenience stores attached that have some food but typically not as large of an inventory as supermarkets and grocery stores.

Cell towers were given a rating of 5 for communications; they were assumed to not provide any additional services.

Emergency muster points like churches and community centers were primarily given a rating of 5 for shelter and safety, with a rating of 4 for communications (assuming that these points would have backup emergency generators to charge phones, for example). These muster points were also given a safety rating of 5, assuming that they would provide access to a safe place to stay during an emergency like a natural disaster, with amenities such as backup power generation for some amount of heating or cooling, blankets, and first aid kits. Additionally, they were given a water rating of 2; some of the facilities have backup water supply (e.g., Estación de Bomberos de Castañer, Escuela Julio Lebron Soto, and Centro Comunal de Castañer were all reported to have water reserves in the emergency planning documents from the Cooperativa. The emergency muster points were also given a medication rating of 2, based on an interview with community leaders from a different energy cooperative in Salinas, Puerto Rico, who reported that the backup generation available in their community center allowed residents to properly refrigerate their medications when they did not have electricity at home. Thus, the rating of 2 reflects the assumption that these sites would provide refrigeration for medications that community members already have, rather than the availability of new medications.

Grocery stores were given a rating of 5 for food and water, and 3 for medications, since, again, they may have over-the-counter medications available; some supermarkets also have pharmacies. We did not have detailed data regarding the availability of medications or a pharmacy at the supermarkets in our list of critical services, so we used the classification of 3 to indicate that they would likely have a larger selection than gas station convenience stores, but they likely would not have as large of an inventory of medications as medical centers such as clinics and hospitals.

Restaurants have played instrumental roles for serving communities experiencing power outages in the past, including in Adjuntas after Hurricane Maria [11], which is why they were included in this list of critical loads. Restaurants were given a rating of 5 and 4 for food and water, respectively.

Medical centers were given a safety and medication rating of 5, with a shelter rating of 4, as shelter is not the primary purpose of medical centers, but it is still an important service that can be provided. Although some medical centers, such as hospitals, serve food and water, these services were not included in the classification list, since other medical centers such as clinics may not have these full services. Medical centers were also assigned a rating of 5 for safety and medications. Farms were given a rating of 5 for food only. Water treatment centers were given a rating of 5 for water supply services.

D. Critical Service Accessibility Characterization

The analysis also requires a characterization of effort required for community members to access the included critical services. In ReNCAT, effort is described by two parameters: a zero distance effort parameter, describing “the effort to acquire this facility’s services, before considering distance,” and an effort per foot parameter, describing “the additional effort to

acquire this facility's services for each foot of distance from the facility's location" [8]. The zero distance parameter can be characterized as the number of hours required for people to travel to the facility. We used the following effort parameter classifications. Both effort parameters were set to be low for transmission facilities, since travel is not required by customers or workers to access those services. The effort parameters for utility facilities are slightly higher, to reflect how effort and time are required for workers to travel to the facility but are not as high as those for in-person facilities, since customers do not have to travel to utility facilities. Finally, the effort parameters for all in-person facilities are much higher, since workers as well as customers must travel to access their services.

TABLE 4.
MODEL INPUTS DESCRIBING EFFORT REQUIRED TO ACCESS CRITICAL SERVICES

Service Category	Description	Included Facilities	Zero Distance	Effort per Foot
Transmission Facilities	Neither customers nor workers need to travel to the facility to access or provide services	Cell towers	0.005	0.005
Utility Facilities	Customers do not need to travel to the facility to access the services, but workers must travel to the facility to provide services	Water treatment facilities	0.01	0.01
In-person Facilities	Customers and workers must travel to the facility to access and provide services	Gas stations, grocery stores, restaurants, medical centers, emergency muster points	0.4	0.05

E. Microgrid and Switch Location Selection

One objective of this analysis was to determine if it would be advantageous to split each feeder network into a series of microgrids with their own independent generation assets and served loads. These microgrids would be formed by using existing switches or installing new switches along the feeder. We did not have data for existing switches in the feeder for the Cordillera Central, so we selected switch locations considering both electrical load and vulnerability of each section of the feeder line to damage from dense vegetation cover. For electrical load, we tried to select switch locations that would generally divide the feeder into sections with around the same number of customers served by each. We also placed switches in a way that would not have too many critical loads reliant on one section of the feeder, in case that section's microgrid were to experience any issues resulting in an outage. For the consideration of tree canopy cover, we used the National Land Cover Database Tree Canopy Cover information to overlay spatial qualitative tree cover density estimates with the feeder [12]. Figure 33 illustrates the switch locations.

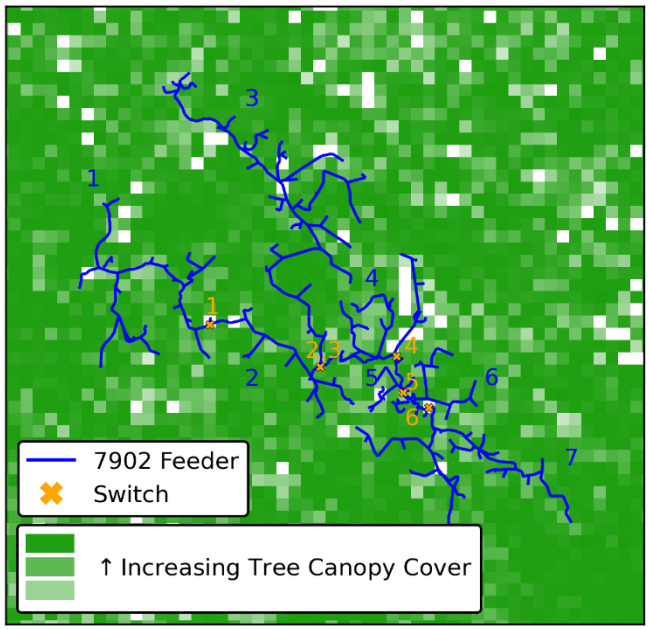

Figure 33. Switch Location Selection

The intention was to identify less densely vegetated areas in which switchgear would be at lower risk of damage from falling trees, wildfires, and other vegetation-related hazards.

The switch location selection for 6 switches led to the establishment of 7 distinct power lines. We specified that all power lines were disconnect-eligible except for Line 6, which is located in the town of Castañer and is connected to multiple critical facilities that cover many necessary services, including a supermarket, several emergency muster points, several cell towers, and a hospital. The switch location information is provided in Table 5.

TABLE 5.
SWITCH LOCATIONS

Switch	Bus	Latitude	Longitude
1	19497512	18.1962	-66.8785
2	19496470	18.18705	-66.8537
3	19496470	18.18705	-66.8537
4	19499708	18.1893	-66.8365
5	19562776	18.18158	-66.835
6	19498850	18.17841	-66.8292

F. Disconnect Costs

The ReNCAT analysis requires the estimation of costs for disconnecting noncritical loads and critical loads from the lines to which they are connected, as well as the costs for opening or closing switches between power lines within the overall feeder. It was assumed that no switches are currently present in locations in which they are assumed to be present for this analysis; thus, we needed to estimate opening costs for the installation of automated and remotely controlled reclosers. Based on discussions with procurement experts at Sandia National Laboratories regarding recloser sizing and pricing, and considering compliance requirements with the Build America, Buy America (BABA) Act [13], we assumed a cost of $60,000 for installing the required reclosers, including relay installation for control purposes and labor hours. We assumed that the same type of recloser would be installed for groups of noncritical loads on each power line, individual critical loads, and on power lines, for ease of maintenance and part replacement, even if this assumption would mean overestimating some sizes and costs for smaller loads along the feeder.

G. Energy Generation Assets

We specified discrete energy generation asset capacity options based on the OpenDSS distribution models developed for Feeder 7902. Although the type of energy generation does not matter for the ReNCAT analysis (only the capacity is included in the optimization), these energy assets were all assumed to be photovoltaic panels.

The two size options for energy generation were 100 kW and 450 kW. ReNCAT also accounts for the costs of installing discrete energy generators; one review estimated that, in 2025, the cost of solar panels in San Juan was around $3/W, so this number was used to calculate overall costs of each energy generation asset ($300k and $1.35M for each 100 kW and 450 kW solar installation, respectively) [14].

H. Population Data

ReNCAT uses the characteristics of the population served by the feeder to determine the impacts of powering and un-powering certain loads along the feeder. Census block information from the 2020 Census was the most granular information found [15].

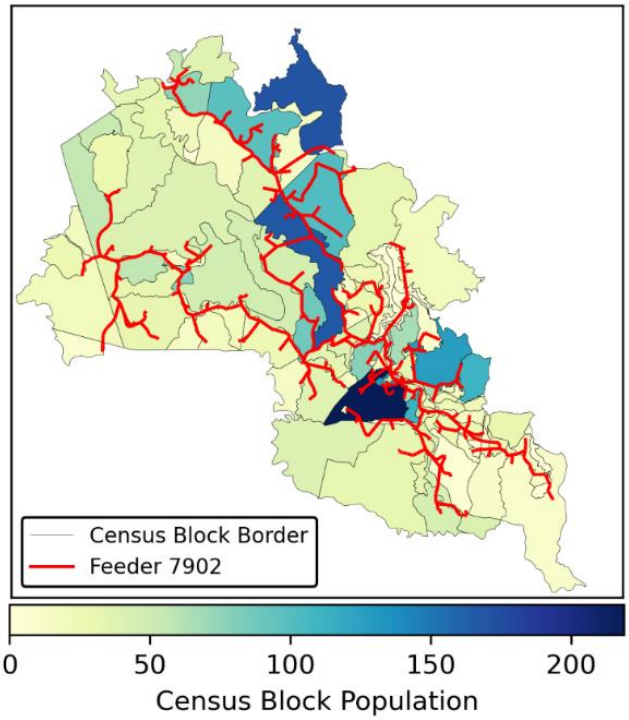

Figure 34. Populations of Census Blocks in Study Area

ReNCAT also requires assignment of an attainment factor to each geographic location in the model. This attainment factor represents the relative ability of each group of people to access critical services during an emergency. We used the median annual income from Census Table S1903, in 2023 inflation-adjusted dollars, as the attainment factor for this model [16].

I. Resilience Assessment Results

The results of the resilience assessment, in the form of a portfolio of options for switch opening locations, number of each discrete generators of each size to purchase, and recommendations for critical services to keep powered and unpowered during typical DBTs, are provided as a Pareto curve in Figure 33.

Higher ReNCAT metric numbers indicate a higher effort required of the population to access critical services, and/or a lower ability of the population to access critical services.

While the costs are estimates and the ReNCAT metric is an approximate number quantifying and describing the community benefits of improving access to certain critical services, the Pareto curve demonstrates differences in the impact of investment into a microgrid system at different scales on a community. Some investment options may require a small investment for a large improvement in community access to critical services. For example, the leftmost point on the graph represents the lowest-cost investment option but the highest burden relative to all the investment options and selecting an investment option around a quarter of a million dollars more can lead to over a 40% reduction in the ReNCAT metric. In other cases where the slope of the Pareto curve is shallower, investing more in a different microgrid solution may not lead to

enough of an improved ReNCAT metric to justify the greater costs.

These results can be used as a foundation for factoring in resilience when developing and constructing a microgrid serving the loads of the 7902-01 feeder network. Budget numbers can be used to eliminate options that are estimated to be out of range, and further analyses such as rooftop solar space availability or ground-mounted solar land availability can help refine which solutions are best for the community.

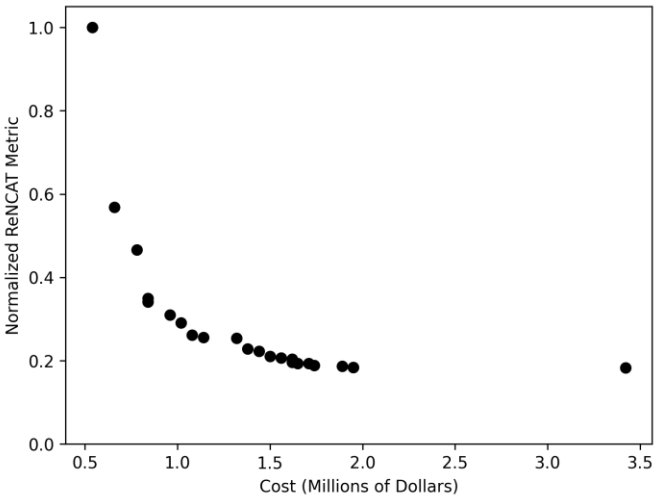

Figure 35. Pareto Curve of Solutions for Microgrid Resilience

V. Qualitative Risk Assessment

Safety risk assessment methods can be used to characterize and understand hazards, causes, consequences, and hazards and threats to a system, as well as their causes and consequences. This information can be used to identify and consider possible hazard and consequence mitigations. Qualitative risk assessment in particular can help understand safety risks at a high level during early stages of planning and design of a system, because some mitigations may be useful to implement in the system design before it has been constructed and before operation has commenced. We conducted a qualitative risk assessment using hazard and operability analysis (HAZOP) methods, applied to electrical system components, to identify hazards and mitigations for microgrid equipment.

A. Hazard and Operability Analysis (HAZOP) Methods

HAZOP methods are used to understand deviations from normal operation and the potential causes and consequences of those deviations [17]. While HAZOPs are typically used for chemical or other industrial processes, the methods are still useful for understanding hazards in other types of systems, hence the application to an electrical system in this study.

First, the scope of the system was defined. The first type of equipment we included was the feeder or distribution lines (i.e., medium-voltage lines transmitting electricity between transformers for larger-scale transmission lines, and transformers going to the point of use) and secondary lines (i.e., low-voltage lines transmitting electricity directly to the point of use). PV generation assets and ancillary equipment (transformers and switchgear) was also included. The main switchgear of interest were reclosers, both as part of overhead lines and at the level of individual facilities that can connect and disconnect at the main grid, for example, critical facilities that may have their own backup generators and elect to disconnect from the grid in the event of an anticipated power outage or other grid disturbance.

Next, we selected guide words as prompts for identifying system deviations. Typical HAZOP guide words include “no,” “more,” “less,” “part of,” “as well as,” “reverse,” “other than,” “early,” “late,” “before,” and “after,” to indicate qualitative and relative deviations to normal process operations in terms of amounts of different relevant parameters, time, and sequence or order of events. We used guide words “no,” “reverse,” “less,” “more,” “as well as,” and “other” for this HAZOP. “No” was used to indicate deviations such as complete loss of power through the system and lack of system operation when needed (such as when trips or faults are expected or needed). “Reverse,” was used to indicate electricity flows in directions for which the line was not designed to handle. “Less” was used to indicate deviations such as material losses in PV modules resulting in adverse outcomes like power output losses. “More” was used to indicate deviations such as overcurrent through the electrical equipment. “As well as” was used to refer to deviations in which contaminants may be introduced to the system (i.e., contaminants are present in the vicinity of the equipment). “Other” was used to indicate any other deviation not covered by the guide words.

Note that this HAZOP is not comprehensive; it does not consider all equipment nor all deviations that may occur for microgrid equipment. It is meant to provide a starting point for identifying deviations and mitigations. It can be used in conjunction with future quantitative risk assessments to characterize and rank risks and mitigation strategies in more detail, especially when prioritizing mitigation strategies based on factors like cost and effectiveness.

B. Risk Assessment Results

The findings of the risk assessment are presented in Table *VI*. General wear and aging of components over time can certainly lead to electrical, thermal, and mechanical hazards such as short circuits in transformer equipment. The more place-specific and system-specific deviations may provide more unique insights – for example, the environmental conditions such as weather and tree cover may impact electrical components such as power lines and PV generation assets. For many of these hazards, ensuring longevity of the system components and promoting reliable and resilient operation can be achieved through a combination of siting selection, microgrid hardening through design as well as establishment of rigorous operation, inspection, and maintenance protocols.

Comparing consequence frequencies and mitigation costs were outside of the scope of this work, but they are also important considerations for prioritizing mitigations. For example, the Cordillera Central region has historically experienced both earthquakes and heavy wind and rain

conditions from hurricanes, but the frequency and future probability of impact from each of those natural disasters may not be equal. Thus, hardening strategies for the most relevant hazards can be prioritized. Similarly, specific mitigation costs, along with other considerations of resources like available staff and time constraints, can be used to determine the value of each mitigation strategy. For example, remote monitoring of power output from PV generation assets can be greatly helpful for identifying potential issues in the system, as well as tracking the overall production for reporting purposes. Resources needed for monitoring must be considered – for example, Internet connection may be required, which may not always be available, especially in conjunction with hazards that can damage the system itself. Staff and/or analytical tools may also be needed to process the monitored information in a usable format; otherwise, the insights may not be as beneficial as planned. It is also noteworthy that some of the mitigations and considerations for those mitigations are repeated between deviations. Clustered benefits of different mitigation strategies may also provide additional justification for implementation.

Safety risk is only one aspect of a microgrid project that can influence design and operation protocols, and it can be considered in tandem with other project parameters such as funding availability, community perception and feedback, reporting needs, permitting or licensing regulations, and future goals for the project. Engaging stakeholders such as authorities having jurisdiction, community members, and industry manufacturers can help justify and select different risk mitigation strategies for a microgrid system.

TABLE *VI*.
RISK ASSESSMENT RESULTS

Component	Guide Word	Deviation	Causes	Possible Consequences	Mitigations	Considerations for Mitigations
Power lines	No	No/loss of power flow	• Tree impacts (e.g., fallen trees, wildfire spread) • Heavy winds • Heavy rain • Environmental conditions may impact both the power lines themselves as well as the poles to which they are mounted	• Unpowering of / loss of access to critical facilities	• Use underground lines where possible [18] • Implement a vegetation maintenance plan [18] • For any new overhead power line and/or power poles installations, select locations that are easy to access for equipment and vegetation maintenance [18] • Use metal power poles rather than wooden power poles to increase integrity/strength [18] • For wooden power poles, ensure that poles are monitored for integrity issues and replaced/ updated when necessary [18] • Reinforce power poles [18]	• While some microgrids do not require installation of any power lines (for example, residential or block-scale microgrids), a regional microgrid likely will require the use of power lines between generation assets and loads • Undergrounding lines is more costly and time-consuming to construct than using overhead lines; permitting and other legal permissions may also take longer • Vegetation maintenance and reinforcement of existing power lines and poles is likely the most attainable and affordable action in the short-term

Component	Guide Word	Deviation	Causes	Possible Consequences	Mitigations	Considerations for Mitigations
	Reverse	Electrical flow (bidirectional flow along feeder line)	• Mismatch between energy generation and utility-level usage	• Electrical damage to feeder lines	• Install anti-islanding devices at points of interconnection between microgrids and the feeder lines [19] • Implement battery storage to manage/control energy arbitrage [19]	• Control equipment, including anti-islanding devices and smart inverters, are also required by LUMA [20] • Control equipment may be costly; need to figure out how cost sharing will work with the different ratepayers in the system [19]
	No	No faulting or tripping of isolated microgrids when needed/ expected	• Possibility of tripping setpoints not being met when needed due to inclusion of variable energy generators in system	• Dangerous conditions for operators and/or maintenance personnel intending to perform work on a de-energized system [19]	• Install anti-islanding devices at points of interconnection between microgrids and the feeder lines [19]	• Control equipment, including anti-islanding devices and smart inverters, are also required by LUMA [20] • Control equipment may be costly; need to figure out how cost sharing will work with the different ratepayers in the system [19]
PV assets	No	Connection (disconnection) of electrical components on PV panels	• Earthquake or other seismic activity	• Generation downtime, potentially during times when other generation assets have also lost function • Unexpected maintenance needs and associated costs	• Use friction-based mounting materials (e.g., rubber) for rooftop solar mounting [18] • Use flexible racking for ground-mounted solar [18]	• Rooftop friction-based mounting feasibility depends on the roof material

Component	Guide Word	Deviation	Causes	Possible Consequences	Mitigations	Considerations for Mitigations
	Less	Insulation resistance	• Flooding / water / moisture impacts on solar panels (e.g., from hurricanes, other heavy rainstorms, or riverine flooding)	• Leakage voltage • Reduction in energy production	• Use drainage (e.g., gutters on rooftops or site drainage for ground-mounted solar) to prevent water accumulation and ingress into areas containing electronics related to PV assets [18] • Siting (e.g., select sites outside of the FEMA Special Flood Hazard Area and/or elevate ground-mounted panels above the floodplain) [18]	• Parts of the Cordillera Central region near Lago Guayo (including near the east side of the town of Castañer) are considered FEMA-designated SFHAs [21]
	Less	Passivation	• Flooding / water / humidity / moisture impacts on solar panels (e.g., from hurricanes or other heavy rainstorms)	• Degradation of power output	• Use drainage (e.g., gutters on rooftops or site drainage for ground-mounted solar) to prevent water accumulation and ingress into areas containing electronics related to PV assets [18] • Siting (e.g., select sites outside of the FEMA Special Flood Hazard Area and/or elevate ground-mounted panels above the floodplain) [18]	• Siting will also depend on other factors including land permitting and ownership, cost, and space availability/constraints
	Other	Discoloration, swelling, or other degradation of encapsulant	• High humidity conditions	• Delamination of interfacial surfaces of PV modules and hot-spot formation that could lead to further delamination [22] • Power degradation	• Conduct routine inspections of solar panels for damages and/or delamination and determine whether repair or replacement may be needed • Monitor power production to identify potential unexpected power output reduction	• Remote/smart monitoring of power production requires Internet connection, which may not always be available, especially during or after a hurricane

Component	Guide Word	Deviation	Causes	Possible Consequences	Mitigations	Considerations for Mitigations
	More	Accelerated corrosion of PV module metal materials	• High humidity and high temperature conditions	• Increase in series resistance • Deterioration of fill factor • Reduction of power output	• Select solar panels with monocrystalline PV systems rather than amorphous PV systems to protect against high humidity / high temperature combination condition [18]	• Selection of solar panel type will also depend on other factors, including cost, availability, and repair/maintenance capabilities
	Other	Breakage of PV cover glass	• High winds resulting in impacts with other objects (e.g., during hurricanes or other strong-wind storms)	• Downtime and potential costs of replacing panels	• The probability of catastrophic damage resulting in no power output is low because of solar panel design • Inspection of solar panels after a storm and monitoring of power output is likely sufficient for maintaining awareness of the state of the solar system	• The Bloomberg New Energy Finance Corporation (NEF) list of "Tier 1" solar module manufacturers can be used to select PV modules with vetted warranties [23, p. 1]
	Less	Integrity of solar panel infrastructure (e.g., fatigue damage or even collapse of solar panels)	• High wind conditions	• Downtime and potential costs of replacing panels	• Siting (e.g., placement of PV assets at the bottom of a hill rather than the top) [18] • Bold/mount modules on rails to prevent wind impacts [18]	• Siting will also depend on other factors, including land permitting and ownership, cost, and space availability/constraints
Transformers	As well as	Introduction of water/moisture into transformer oil [24]	• Storm (flooding and/or precipitation) conditions	• Power failure (potentially resulting in loss of failure for all customers, critical and noncritical, downstream of transformer)	• Monitor transformer oil health continuously	• Continuous monitoring systems require Internet (which may not always be available, especially during or after a hurricane, which may also be when transformer oil is at a higher risk of experiencing moisture ingress)

Component	Guide Word	Deviation	Causes	Possible Consequences	Mitigations	Considerations for Mitigations
	More	Current (overcurrent)	• Aging transformer infrastructure	• Short-circuiting and tripping or even complete failure of the transformer • Potential thermal impacts (e.g., fire)	• Inspect and periodically update/maintain transformer infrastructure	• Includes new transformers as well as transformers on the existing electrical system
Switchgear	As well as	Introduction of water/moisture into switchgear	• Storm (flooding and/or precipitation) conditions	• Corrosion of metal parts, resulting in compromised component integrity and/or • Potential short-circuiting and associated outcomes (e.g., thermal impacts and fire; electrical failure)	• House switchgear in enclosures (provide shelter at the very least, and can also additionally provide environmental – e.g., temperature and humidity – control if needed) • Monitor and control switchgear using remotely controlled relays	• Switchgear enclosures with more capabilities (e.g., environmental control) will be more expensive and may require more maintenance (also energy usage would need to be accounted for) • Switchgear enclosure needs also greatly depend on the size of the switchgear • Remote/smart monitoring of switchgear function requires Internet connection, which may not always be available, especially during or after a hurricane

ACKNOWLEDGMENTS

This research was supported in part by the U.S. Department of Energy (DOE) under grant number xxxxxxxxxxxxxxx.

This article has been authored by an employee of National Technology & Engineering Solutions of Sandia, LLC under Contract No. DE-NA0003525 with the U.S. Department of Energy (DOE). The employee owns all rights, title and interest n and to the article and is solely responsible for its contents. The U.S. Government retains and the publisher, by accepting the article for publication, acknowledges that the U.S. Government retains a non-exclusive, paid up, irrevocable, world-wide license to publish or reproduce the published form of this article or allow others to do so, for U.S. Government purposes. The DOE will provide public access to these results of federally sponsored research in accordance with the DOE Public Access Plan.

Sandia National Laboratories is a multimission laboratory managed and operated by National Technology & Engineering Solutions of Sandia, LLC, a wholly owned subsidiary of Honeywell International, Inc., for the U.S. Department of Energy's National Nuclear Security Administration under contract DE-NA0003525.

REFERENCES

[1] T.-T. Ku, C.-H. Lin, C.-S. Chen, and C.-T. Hsu, "Coordination of Transformer On-Load Tap Changer and PV Smart Inverters for Voltage Control of Distribution Feeders," *IEEE Transactions on Industry Applications*, vol. 55, no. 1, pp. 256–264, 2018.

[2] R. Kabiri, D. G. Holmes, B. P. McGrath, and L. Meeghapola, "LV Grid Voltage Regulation Using Transformer Electronic Tap Changing, With PV Inverter Reactive Power Injection," *IEEE Journal of Emerging and Selected Topics in Power Electronics*, vol. 3, no. 4, pp. 1182–1192, 2015.

[3] Y. P. Agalgaonkar, B. C. Pal, and R. A. Jabr, "Distribution Voltage Control Considering the Impact of PV Generation on Tap Changers and Autonomous Regulators," *IEEE*

Transactions on Power Systems, vol. 29, no. 1, pp. 182–192, 2013.

[4] Y. Maataoui, H. Chekenbah, O. Boutfarjoute, V. Puig, and R. Lasri, "A Coordinated Voltage Regulation Algorithm of a Power Distribution Grid with Multiple Photovoltaic Distributed Generators Based on Active Power Curtailment and On-Line Tap Changer," *Energies*, vol. 16, no. 14, p. 5279, 2023.

[5] M. Chamana and B. H. Chowdhury, "Impact of Smart Inverter Control with PV Systems on Voltage Regulators in Active Distribution Networks," in *2014 11th Annual High Capacity Optical Networks and Emerging/Enabling Technologies (Photonics for Energy)*, Institute of Electrical and Electronics Engineers, 2014, pp. 115–119.

[6] A. Neupane and S. Paudyal, "Dynamic Droop Setting of Smart Inverters in Active Distribution Grid Using Neural Networks," in *2024 56th North American Power Symposium (NAPS)*, Institute of Electrical and Electronics Engineers, 2024, pp. 1–6.

[7] *PVWatts Calculator*. (Mar. 2025). National Renewable Energy Laboratory. [Online]. Available: https://pvwatts.nrel.gov

[8] D. Melander and A. M. Wachtel, "ReNCAT 2.2 User Manual," Sandia National Laboratories, Apr. 2024.

[9] U.S. National Geospatial-Intelligence Agency, "Puerto Rico Cell Towers." 2022. Accessed: Sep. 30, 2025. [Online]. Available: https://koordinates.com/layer/110898-puerto-rico-cell-towers/

[10] Energy Star, "U.S. Energy Use Intensity by Property Type." 2024. [Online]. Available: https://portfoliomanager.energystar.gov/pdf/reference/US%20National%20Median%20Table.pdf

[11] K. Rapin, "Community-Powered Solar in Puerto Rico," *yes!*, Jun. 13, 2023. [Online]. Available: https://www.yesmagazine.org/environment/2023/06/13/puerto-rico-solar-power

[12] U.S. Forest Service, "National Land Cover Database (NLCD) Tree Canopy Cover (TCC) Puerto Rico USVI." May 06, 2024. doi: 10.5066/P94UXNTS.

[13] "Build America, Buy America," U.S. Environmental Protection Agency. [Online]. Available: https://www.epa.gov/baba/build-america-buy-america-baba-overview

[14] A. Sendy, "Solar Panel Cost San Juan: Prices and Data 2025," Solar Reviews. [Online]. Available: https://www.solarreviews.com/solar-panel-cost/puerto-rico/san-juan

[15] U.S. Census Bureau, "Total Population."

[16] U.S. Census Bureau, "Median Income in the Past 12 Months (in 2023 Inflation-Adjusted Dollars)."

[17] P. Mocellin *et al.*, "Experimental methods in chemical engineering: Hazard and operability analysis - HAZOP," *The Canadian Journal of Chemical Engineering*, vol. 100, no. 12, pp. 3450–3469, Jun. 2022, doi: 10.1002/cjce.24520.

[18] R. Darbali-Zamora, M. Louie, J. Choi, and J. D. Flicker, "Quantification of Harsh Environments, At-Risk Microgrid Components, and Hardening Technologies," Sandia National Laboratories, Publication in Progress.

[19] M. S. Louie and R. Darbali-Zamora, "Regulatory and Technical Challenges and Barriers to Adoption of Distributed Wind Energy in Agricultural Settings," Sandia National Laboratories, Publication in Progress.

[20] "Smart Inverter Settings Sheets." LUMA, Nov. 15, 2024. [Online]. Available: https://lumapr.com/wp-content/uploads/2024/12/2024.11.15_Technical-Bulletin_2024-0001_Smart_Inverter_Settings_Sheet-1.pdf

[21] "FEMA's National Flood Hazard Layer (NFHL) Viewer," Federal Emergency Management Agency. [Online]. Available: https://hazards-fema.maps.arcgis.com/apps/webappviewer/index.html?id=8b0adb51996444d4879338b5529aa9cd

[22] R. Meena, A. Pareek, and R. Gupta, "A comprehensive Review on interfacial delamination in photovoltaic modules," *Renewable and Sustainable Energy Reviews*, vol. 189, p. 113944, Jan. 2024, doi: 10.1016/j.rser.2023.113944.

[23] "Tier 1 Solar Module Maker Methodology." Bloomberg New Energy Finance Corporation, Jul. 09, 2025. [Online]. Available: https://assets.bnef.com/public/tiering/solarmodules.pdf

[24] M. Fahad Naveed, A. Amaar, S. Saleem Khan, M. Omar, and S. Larkin, "Detection and continuous monitoring of moisture content in transformer oil using fractal-based capacitive sensor," *Heliyon*, vol. 10, no. 24, p. 40995, Dec. 2024.

VI. Appendix

A. Appendix A: Resilience Study Additional Materials

TABLE *VII*.
CENSUS BLOCK INFORMATION FOR RESILIENCE STUDY AREA

Tract	Block	Lat.	Long.	Median Income	Pop.
9563	1030	18.20127	-66.76774	17269	17
9564	2000	18.20866	-66.8258	22279	19
9564	2009	18.18512	-66.82356	22279	127
9564	2010	18.17947	-66.82895	22279	14
9564	2011	18.19193	-66.82673	22279	9
9564	2012	18.19704	-66.83275	22279	0
9564	2013	18.20685	-66.83365	22279	0
9564	2014	18.18321	-66.83127	22279	34
9564	2015	18.18056	-66.83158	22279	18
9564	2016	18.18015	-66.83066	22279	0
9564	2017	18.19061	-66.83204	22279	66
9564	2018	18.18635	-66.83112	22279	25
9564	2019	18.19376	-66.83305	22279	4
9564	2020	18.1782	-66.82581	22279	66
9564	2021	18.17582	-66.82595	22279	17
9564	2022	18.1787	-66.82147	22279	12
9564	2023	18.18133	-66.81579	22279	111
9564	2025	18.17666	-66.81471	22279	8
9564	2026	18.17568	-66.81887	22279	14
9564	2027	18.17655	-66.82279	22279	23
9564	2028	18.17785	-66.81966	22279	14
9564	2029	18.16938	-66.82319	22279	25
9564	2030	18.17001	-66.81896	22279	24
9564	2031	18.16834	-66.81851	22279	9
9564	2032	18.17255	-66.81789	22279	15
9564	2034	18.17508	-66.81536	22279	22
9564	2036	18.16002	-66.82057	22279	5
9564	2037	18.16526	-66.81735	22279	9
9564	2038	18.16577	-66.81517	22279	7
9564	2039	18.17472	-66.82123	22279	23
9564	2040	18.18339	-66.8341	22279	9
9565	2023	18.17114	-66.81256	16875	16
9565	2024	18.1669	-66.81299	16875	6
9565	2025	18.17015	-66.80731	16875	30
9565	2032	18.15053	-66.80059	16875	9

9565	2033	18.15616	-66.79965	16875	0
9565	2034	18.16599	-66.8103	16875	21
9565	2035	18.15644	-66.8125	16875	11
9565	2036	18.16229	-66.80214	16875	13
9565	2037	18.16787	-66.80221	16875	0

TABLE *VIII*.
CENSUS BLOCK INFORMATION FOR RESILIENCE STUDY AREA

Tract	Block	Lat.	Long.	Median Income	Pop.
9583	1015	18.23082	-66.8823	18125	0
9583	1012	18.23245	-66.85834	18125	15
9583	2030	18.24454	-66.88231	18125	75
9583	2032	18.2075	-66.88462	18125	14
9583	2015	18.23868	-66.88969	18125	32
9583	1019	18.25093	-66.88563	18125	53
9583	2023	18.22819	-66.89426	18125	37
9583	2026	18.22304	-66.90671	18125	56
9583	1011	18.23838	-66.86843	18125	98
9583	2028	18.21724	-66.88561	18125	40
9583	1013	18.22388	-66.86662	18125	35
9583	2029	18.23722	-66.88357	18125	18
9583	1006	18.25173	-66.87783	18125	36
9583	1008	18.24292	-66.85478	18125	170
9583	2024	18.23649	-66.90348	18125	53
9583	2016	18.24528	-66.8966	18125	34
9583	2031	18.20576	-66.89386	18125	57
9583	1014	18.23147	-66.8751	18125	16
9583	2025	18.22916	-66.9011	18125	28
9584	1002	18.20278	-66.84993	15582	167
9584	2008	18.18129	-66.83401	15582	66
9584	2003	18.18471	-66.83758	15582	23
9584	2014	18.17918	-66.85878	15582	14
9584	1003	18.2018	-66.84658	15582	15
9584	2018	18.17397	-66.83015	15582	112
9584	2007	18.18022	-66.83652	15582	130
9584	1013	18.20209	-66.84509	15582	12
9584	1004	18.2069	-66.86002	15582	45
9584	1001	18.22062	-66.85126	15582	101
9584	1008	18.20345	-66.88441	15582	77
9584	1010	18.19387	-66.89224	15582	31
9584	1021	18.18902	-66.83632	15582	12
9584	2020	18.17452	-66.82856	15582	57
9584	2011	18.18192	-66.83309	15582	17
9584	2015	18.18842	-66.8632	15582	25
9584	2013	18.18502	-66.84972	15582	33
9584	2002	18.18434	-66.83551	15582	0
9584	2022	18.17117	-66.83549	15582	3
9584	1012	18.19127	-66.87698	15582	17
9584	1022	18.18952	-66.84495	15582	39
9584	2009	18.17702	-66.83092	15582	66
9584	2000	18.18536	-66.84131	15582	79
9584	1007	18.19795	-66.88376	15582	13
9584	1015	18.19944	-66.8368	15582	13
9584	1020	18.19925	-66.84663	15582	13
9584	1018	18.19444	-66.84399	15582	11
9584	1000	18.21891	-66.83969	15582	32
9584	1019	18.19838	-66.84143	15582	28
9584	2017	18.19391	-66.87249	15582	20
9584	1024	18.19357	-66.85456	15582	88
9584	2012	18.17777	-66.85204	15582	37
9584	1014	18.20348	-66.84078	15582	23
9584	2021	18.1721	-66.82733	15582	24
9584	2019	18.17654	-66.82759	15582	25
9584	2010	18.17919	-66.83068	15582	38
9584	1017	18.19433	-66.83779	15582	19
9584	2006	18.17386	-66.84613	15582	9
9584	1011	18.19034	-66.88316	15582	13
9584	1009	18.20076	-66.88949	15582	31
9584	2023	18.18077	-66.8356	15582	55
9584	1005	18.204	-66.8648	15582	46
9584	2016	18.19313	-66.86844	15582	18
9584	1006	18.20298	-66.8736	15582	47
9584	2001	18.18437	-66.83955	15582	9
9584	2005	18.17584	-66.83988	15582	219
9584	2004	18.18054	-66.84542	15582	14
9584	1023	18.18834	-66.84305	15582	4
9584	1016	18.20034	-66.83607	15582	0

TABLE *IX*.
CENSUS BLOCK INFORMATION FOR RESILIENCE STUDY AREA

Tract	Block	Lat.	Long.	Median Income	Pop.
9597	1053	18.21254	-66.91433	17905	0
9597	1045	18.19774	-66.90934	17905	19
9597	1052	18.2081	-66.91185	17905	27
9597	1047	18.21351	-66.90851	17905	18
9597	1054	18.20825	-66.90727	17905	0
9601	2001	18.1881	-66.90874	20042	8
9601	1015	18.16545	-66.85189	20042	40
7501	1001	18.15089	-66.82435	24297	43
7501	1003	18.15907	-66.82813	24297	31
7501	1002	18.1586	-66.837	24297	32
7501	1000	18.1482	-66.81729	24297	41

B. Appendix B: Resilience Study Detailed Solutions

TABLE *X*.
RESILIENCE STUDY DETAILED SOLUTIONS

Solution	Cost (Millions of Dollars)	Open Switches	Connected Facilities	# of 100 kW PV Systems	# of 450 kW PV Systems
1	0.54	1, 4	• Capilla Virgen de la Medalla Milagrosa Bartolo • Centro de Apoyo Mutuo Bartolo • Gasoline Garage • Iglesia Episcopal Misión San Bartolome Apostol • Lares Medical Center	1	0
2	0.66	4	• Capilla Virgen de la Medalla Milagrosa Bartolo • Centro de Apoyo Mutuo Bartolo • Colmado y Gasolinera Serrano • Gasoline Garage • Iglesia de los Hermanos en Jesucristo • Iglesia Episcopal Misión San Bartolome Apostol • Tanque Alemañy	1	0
3	0.78	4	• Capilla Virgen de la Medalla Milagrosa Bartolo • Centro de Apoyo Mutuo Bartolo • Colmado y Gasolinera Serrano • Gasoline Garage • Here I Stay • Iglesia de los Hermanos en Jesucristo • Iglesia Episcopal Misión San Bartolome Apostol • Lares Medical Center • Tanque Alemañy	2	0
4	0.84	1, 5	• Capilla Virgen de la Medalla Milagrosa Bartolo • Cell Tower 1 • Centro de Apoyo Mutuo Bartolo • Colmado y Gasolinera Serrano • Escuela Julio Lebron Soto • Estación de Bomberos de Castañer • Iglesia Episcopal Misión San Bartolome Apostol • La Profe's NutriStop & Go • Lisandra Church • Parroquia Nuestra Señora de la Medalla Milagrosa	2	0
5	0.84	1, 5	• Capilla Virgen de la Medalla Milagrosa Bartolo • Cell Tower 1 • Centro de Apoyo Mutuo Bartolo • Colmado y Gasolinera Serrano • Escuela Julio Lebron Soto • Estación de Bomberos de Castañer • Gasoline Garage • Iglesia Episcopal Misión San Bartolome Apostol • La Profe's NutriStop & Go • Lares Medical Center • Lisandra Church • Parroquia Nuestra Señora de la Medalla Milagrosa	2	0
6	0.96	5	• Capilla Virgen de la Medalla Milagrosa Bartolo • Cell Tower 1 • Centro de Apoyo Mutuo Bartolo • Colmado y Gasolinera Serrano • Escuela Julio Lebron Soto • Estación de Bomberos de Castañer • Gasoline Garage • Iglesia de los Hermanos en Jesucristo • Iglesia Episcopal Misión San Bartolome Apostol • La Profe's NutriStop & Go	2	0

			• Lisandra Church • Parroquia Nuestra Señora de la Medalla Milagrosa • Tanque Alemañy		
7	1.02	5	• Capilla Virgen de la Medalla Milagrosa Bartolo • Cell Tower 1 • Centro de Apoyo Mutuo Bartolo • Colmado y Gasolinera Serrano • Escuela Julio Lebron Soto • Estación de Bomberos de Castañer • Gasoline Garage • Here I Stay • Iglesia de los Hermanos en Jesucristo • Iglesia Episcopal Misión San Bartolome Apostol • La Profe's NutriStop & Go • Lisandra Church • Tanque Alemañy	2	0
8	1.08	5	• Capilla Virgen de la Medalla Milagrosa Bartolo • Cell Tower 1 • Centro de Apoyo Mutuo Bartolo • Colmado y Gasolinera Serrano • Escuela Julio Lebron Soto • Estación de Bomberos de Castañer • Gasoline Garage • Here I Stay • Iglesia de los Hermanos en Jesucristo • Iglesia Episcopal Misión San Bartolome Apostol • La Profe's NutriStop & Go • Lisandra Church • Parroquia Nuestra Señora de la Medalla Milagrosa • Tanque Alemañy • The Tower Juices	3	0
9	1.14	5	• Capilla Virgen de la Medalla Milagrosa Bartolo • Cell Tower 1 • Centro de Apoyo Mutuo Bartolo • Colmado y Gasolinera Serrano • Escuela Julio Lebron Soto • Estación de Bomberos de Castañer • Gasoline Garage • Here I Stay • Iglesia de los Hermanos en Jesucristo • Iglesia Episcopal Misión San Bartolome Apostol • La Profe's NutriStop & Go • Lares Medical Center • Lisandra Church • Parroquia Nuestra Señora de la Medalla Milagrosa • Tanque Alemañy • The Tower Juices	3	0
10	1.32	1, 6	• Capilla Virgen de la Medalla Milagrosa Bartolo • Castañer Bakery • Cell Tower 1 • Cell Tower 2 • Cell Tower 3 • Cell Tower 4 • Centro Comunal de Castañer • Centro de Apoyo Mutuo Bartolo • Colmado y Gasolinera Serrano • Escuela Julio Lebron Soto • Escuela Superior Gabriela Mistral • Estación de Bomberos de Castañer	3	0

			• Gasoline Garage • Iglesia del Señor de Unción, Poder y Fuego • Iglesia Episcopal Misión San Bartolome Apostol • La Profe's NutriStop & Go • Lisandra Church • Misión la Santa Cruz • Parroquia Nuestra Señora de la Medalla Milagrosa • Policia de Puerto Rico – Precincto Castañer • Seventh Day Adventist Church Castañer		
11	1.38	1	• Capilla Virgen de la Medalla Milagrosa Bartolo • Cell Tower 1 • Cell Tower 2 • Cell Tower 3 • Cell Tower 4 • Centro Comunal de Castañer • Centro de Apoyo Mutuo Bartolo • Colmado y Gasolinera Serrano • Escuela Julio Lebron Soto • Escuela Superior Gabriela Mistral • Estación de Bomberos de Castañer • Gasoline Garage • Hacienda Asunción • Iglesia Bautista de Castañer • Iglesia del Señor de Unción, Poder y Fuego • Iglesia Episcopal Misión San Bartolome Apostol • La Profe's NutriStop & Go • Lisandra Church • Misión la Santa Cruz • Parroquia Nuestra Señora de la Medalla Milagrosa • Policia de Puerto Rico – Precincto Castañer • Seventh Day Adventist Church Castañer	3	0
12	1.44		• Capilla Virgen de la Medalla Milagrosa Bartolo • Castañer Bakery • Cell Tower 1 • Cell Tower 2 • Cell Tower 3 • Cell Tower 4 • Centro Comunal de Castañer • Centro de Apoyo Mutuo Bartolo • Colmado y Gasolinera Serrano • Escuela Julio Lebron Soto • Escuela Superior Gabriela Mistral • Estación de Bomberos de Castañer • Gasoline Garage • Hacienda Asunción • Iglesia Bautista de Castañer • Iglesia del Señor de Unción, Poder y Fuego • Iglesia Episcopal Misión San Bartolome Apostol • La Profe's NutriStop & Go • Lisandra Church • Misión la Santa Cruz • Parroquia Nuestra Señora de la Medalla Milagrosa • Policia de Puerto Rico – Precincto Castañer • Seventh Day Adventist Church Castañer	4	0
13	1.5		• Capilla Virgen de la Medalla Milagrosa Bartolo • Cell Tower 1 • Cell Tower 2 • Cell Tower 3 • Cell Tower 4	3	0

			• Centro Comunal de Castañer • Centro de Apoyo Mutuo Bartolo • Colmado y Gasolinera Serrano • Escuela Julio Lebron Soto • Escuela Superior Gabriela Mistral • Estación de Bomberos de Castañer • Gasoline Garage • Hacienda Asunción • Iglesia Bautista de Castañer • Iglesia de los Hermanos en Jesucristo • Iglesia del Señor de Unción, Poder y Fuego • Iglesia Episcopal Misión San Bartolome Apostol • La Profe's NutriStop & Go • Lisandra Church • Misión la Santa Cruz • Parroquia Nuestra Señora de la Medalla Milagrosa • Policia de Puerto Rico – Precincto Castañer • Seventh Day Adventist Church Castañer • Tanque Alemañy		
14	1.56		• Capilla Virgen de la Medalla Milagrosa Bartolo • Castañer Bakery • Cell Tower 1 • Cell Tower 2 • Cell Tower 3 • Cell Tower 4 • Centro Comunal de Castañer • Centro de Apoyo Mutuo Bartolo • Colmado y Gasolinera Serrano • Escuela Julio Lebron Soto • Escuela Superior Gabriela Mistral • Estación de Bomberos de Castañer • Gasoline Garage • Hacienda Asunción • Iglesia Bautista de Castañer • Iglesia de los Hermanos en Jesucristo • Iglesia del Señor de Unción, Poder y Fuego • Iglesia Episcopal Misión San Bartolome Apostol • La Profe's NutriStop & Go • Lisandra Church • Misión la Santa Cruz • Parroquia Nuestra Señora de la Medalla Milagrosa • Policia de Puerto Rico – Precincto Castañer • Seventh Day Adventist Church Castañer • Tanque Alemañy	4	0
15	1.62		• Capilla Virgen de la Medalla Milagrosa Bartolo • Cell Tower 1 • Cell Tower 2 • Cell Tower 3 • Cell Tower 4 • Centro Comunal de Castañer • Centro de Apoyo Mutuo Bartolo • Colmado y Gasolinera Serrano • Escuela Julio Lebron Soto • Escuela Superior Gabriela Mistral • Estación de Bomberos de Castañer • Gasoline Garage • Hacienda Asunción • Here I Stay • Iglesia de los Hermanos en Jesucristo	4	0

			• Iglesia del Señor de Unción, Poder y Fuego • Iglesia Episcopal Misión San Bartolome Apostol • La Profe's NutriStop & Go • Lisandra Church • Misión la Santa Cruz • Parroquia Nuestra Señora de la Medalla Milagrosa • Policia de Puerto Rico – Precincto Castañer • Seventh Day Adventist Church Castañer • Tanque Alemañy		
16	1.62		• Capilla Virgen de la Medalla Milagrosa Bartolo • Castañer Bakery • Cell Tower 1 • Cell Tower 2 • Cell Tower 3 • Cell Tower 4 • Centro Comunal de Castañer • Centro de Apoyo Mutuo Bartolo • Colmado y Gasolinera Serrano • Escuela Julio Lebron Soto • Escuela Superior Gabriela Mistral • Estación de Bomberos de Castañer • Gasoline Garage • Hacienda Asunción • Here I Stay • Iglesia Bautista de Castañer • Iglesia de los Hermanos en Jesucristo • Iglesia del Señor de Unción, Poder y Fuego • Iglesia Episcopal Misión San Bartolome Apostol • La Profe's NutriStop & Go • Lisandra Church • Misión la Santa Cruz • Parroquia Nuestra Señora de la Medalla Milagrosa • Policia de Puerto Rico – Precincto Castañer • Seventh Day Adventist Church Castañer • Tanque Alemañy	4	0
17	1.65		• Capilla Virgen de la Medalla Milagrosa Bartolo • Cell Tower 1 • Cell Tower 2 • Cell Tower 3 • Cell Tower 4 • Centro Comunal de Castañer • Centro de Apoyo Mutuo Bartolo • Colmado y Gasolinera Serrano • Escuela Julio Lebron Soto • Escuela Superior Gabriela Mistral • Estación de Bomberos de Castañer • Gasoline Garage • Hacienda Asunción • Here I Stay • Iglesia Bautista de Castañer • Iglesia de los Hermanos en Jesucristo • Iglesia del Señor de Unción, Poder y Fuego • Iglesia Episcopal Misión San Bartolome Apostol • La Profe's NutriStop & Go • Lisandra Church • Misión la Santa Cruz • Parroquia Nuestra Señora de la Medalla Milagrosa • Policia de Puerto Rico – Precincto Castañer • Seventh Day Adventist Church Castañer	1	0

			• Tanque Alemañy • The Tower Juices		
18	1.71		• Capilla Virgen de la Medalla Milagrosa Bartolo • Castañer Bakery • Cell Tower 1 • Cell Tower 2 • Cell Tower 3 • Cell Tower 4 • Centro Comunal de Castañer • Centro de Apoyo Mutuo Bartolo • Colmado y Gasolinera Serrano • Escuela Julio Lebron Soto • Escuela Superior Gabriela Mistral • Estación de Bomberos de Castañer • Gasoline Garage • Hacienda Asunción Here I Stay • Iglesia Bautista de Castañer • Iglesia de los Hermanos en Jesucristo • Iglesia del Señor de Unción, Poder y Fuego • Iglesia Episcopal Misión San Bartolome Apostol • Lisandra Church • Misión la Santa Cruz • Parroquia Nuestra Señora de la Medalla Milagrosa • Policia de Puerto Rico – Precincto Castañer • Seventh Day Adventist Church Castañer • Tanque Alemañy • The Tower Juices	1	0
19	1.74		• Capilla Virgen de la Medalla Milagrosa Bartolo • Castañer Bakery • Cell Tower 1 • Cell Tower 2 • Cell Tower 3 • Cell Tower 4 • Centro Comunal de Castañer • Centro de Apoyo Mutuo Bartolo • Colmado y Gasolinera Serrano • Escuela Julio Lebron Soto • Escuela Superior Gabriela Mistral • Estación de Bomberos de Castañer • Gasoline Garage • Hacienda Asunción • Here I Stay • Iglesia Bautista de Castañer • Iglesia de los Hermanos en Jesucristo • Iglesia del Señor de Unción, Poder y Fuego • Iglesia Episcopal Misión San Bartolome Apostol • La Profe's NutriStop & Go • Lares Medical Center • Lisandra Church • Misión la Santa Cruz • Parroquia Nuestra Señora de la Medalla Milagrosa • Policia de Puerto Rico – Precincto Castañer • Seventh Day Adventist Church Castañer • Tanque Alemañy • The Tower Juices	5	0
20	1.89		• Capilla Virgen de la Medalla Milagrosa Bartolo • Castañer Bakery • Cell Tower 1	1	1

			• Cell Tower 2 • Cell Tower 3 • Cell Tower 4 • Centro Comunal de Castañer • Centro de Apoyo Mutuo Bartolo • Colmado y Gasolinera Serrano • Escuela Julio Lebron Soto • Escuela Superior Gabriela Mistral • Estación de Bomberos de Castañer • Gasoline Garage • Hacienda Asunción • Here I Stay • Iglesia Bautista de Castañer • Iglesia de los Hermanos en Jesucristo • Iglesia del Señor de Unción, Poder y Fuego • Iglesia Episcopal Misión San Bartolome Apostol • La Profe's NutriStop & Go • Lisandra Church • Misión la Santa Cruz • Parroquia Nuestra Señora de la Medalla Milagrosa • Policia de Puerto Rico – Precincto Castañer • Seventh Day Adventist Church Castañer • Supermercado Mega Fresh Castañer • Tanque Alemañy • The Tower Juices		
21	1.95		• Capilla Virgen de la Medalla Milagrosa Bartolo • Castañer Bakery • Cell Tower 1 • Cell Tower 2 • Cell Tower 3 • Cell Tower 4 • Centro Comunal de Castañer • Centro de Apoyo Mutuo Bartolo • Colmado y Gasolinera Serrano • Escuela Julio Lebron Soto • Escuela Superior Gabriela Mistral • Estación de Bomberos de Castañer • Gasoline Garage • Hacienda Asunción • Here I Stay • Iglesia Bautista de Castañer • Iglesia de los Hermanos en Jesucristo • Iglesia del Señor de Unción, Poder y Fuego • Iglesia Episcopal Misión San Bartolome Apostol • La Profe's NutriStop & Go • Lares Medical Center • Lisandra Church • Misión la Santa Cruz • Parroquia Nuestra Señora de la Medalla Milagrosa • Policia de Puerto Rico – Precincto Castañer • Seventh Day Adventist Church Castañer • Supermercado Mega Fresh Castañer • Tanque Alemañy • The Tower Juices	1	1
22	1.95		• Capilla Virgen de la Medalla Milagrosa Bartolo • Castañer Bakery • Cell Tower 1 • Cell Tower 2 • Cell Tower 3	1	1

			• Cell Tower 4 • Centro Comunal de Castañer • Centro de Apoyo Mutuo Bartolo • Colmado y Gasolinera Serrano • Escuela Julio Lebron Soto • Escuela Superior Gabriela Mistral • Estación de Bomberos de Castañer • Gasoline Garage • Hacienda Asunción • Here I Stay • Iglesia Bautista de Castañer • Iglesia de los Hermanos en Jesucristo • Iglesia del Señor de Unción, Poder y Fuego • Iglesia Episcopal Misión San Bartolome Apostol • La Profe's NutriStop & Go • Lares Medical Center • Lisandra Church • Misión la Santa Cruz • Parroquia Nuestra Señora de la Medalla Milagrosa • Policia de Puerto Rico – Precincto Castañer • Seventh Day Adventist Church Castañer • Supermercado Mega Fresh Castañer • Tanque Alemañy • The Tower Juices		
23	3.42		• Capilla Virgen de la Medalla Milagrosa Bartolo • Castañer Bakery • Cell Tower 1 • Cell Tower 2 • Cell Tower 3 • Cell Tower 4 • Centro Comunal de Castañer • Centro de Apoyo Mutuo Bartolo • Colmado y Gasolinera Serrano • Escuela Julio Lebron Soto • Escuela Superior Gabriela Mistral • Estación de Bomberos de Castañer • Gasoline Garage • Hacienda Asunción • Here I Stay • Hospital General de Castañer • Iglesia Bautista de Castañer • Iglesia de los Hermanos en Jesucristo • Iglesia del Señor de Unción, Poder y Fuego • Iglesia Episcopal Misión San Bartolome Apostol • La Profe's NutriStop & Go • Lares Medical Center • Lisandra Church • Misión la Santa Cruz • Parroquia Nuestra Señora de la Medalla Milagrosa • Policia de Puerto Rico – Precincto Castañer • Seventh Day Adventist Church Castañer • Supermercado Mega Fresh Castañer • Tanque Alemañy • The Tower Juices	2	2